

三体核反应：转移反应、破裂反应和三核子反应

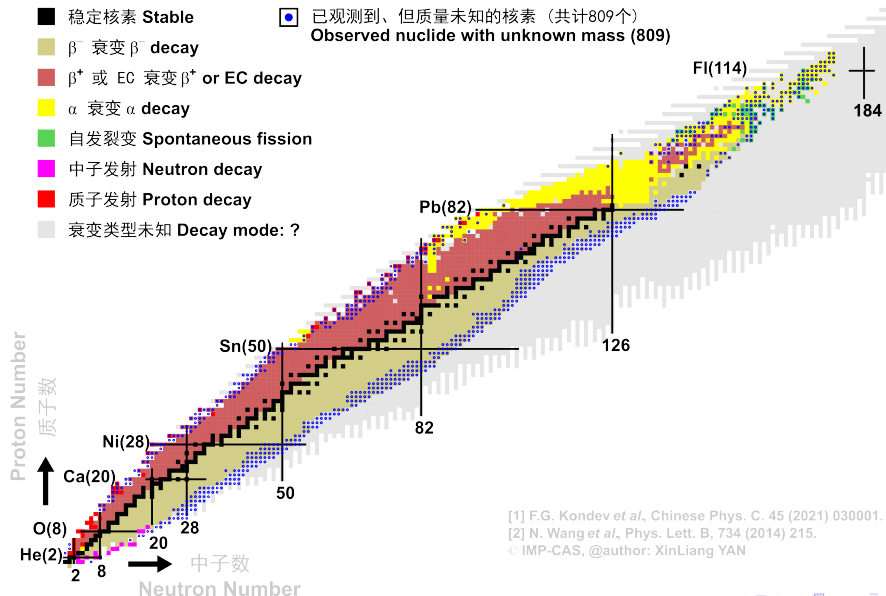
庞丹阳

北京航空航天大学物理学院

2022 年 9 月 30 日

Nuclear Chart: decay mode of the ground state nuclide(NUBASE2020)

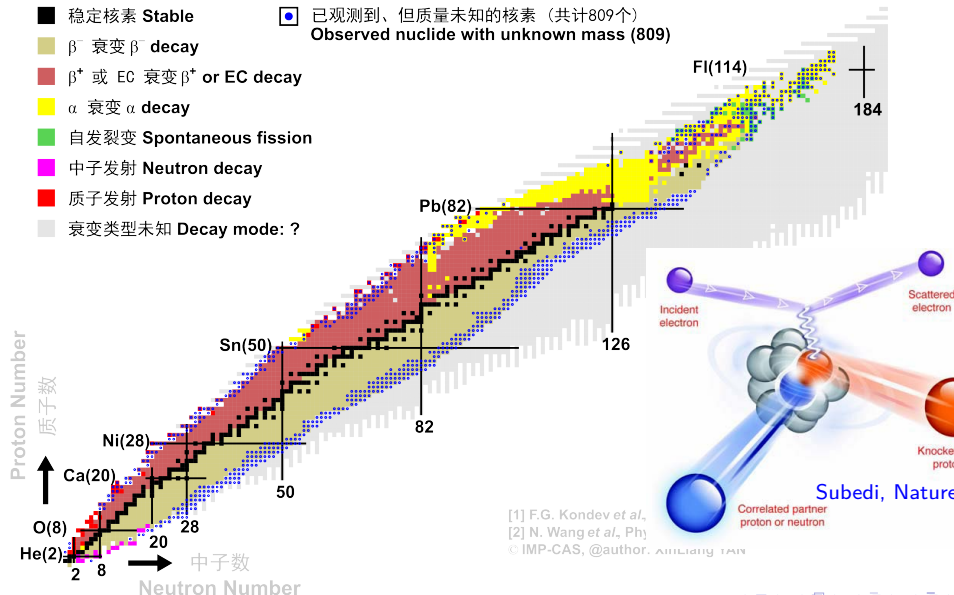
核素图：基态原子核的衰变类型(NUBASE2020)



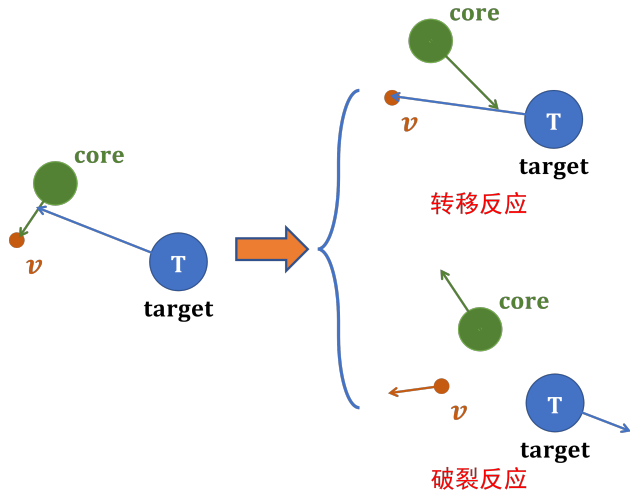
Nuclear Chart: decay mode of the ground state nuclide(NUBASE2020)
 核素图：基态原子核的衰变类型(NUBASE2020)

- 稳定核素 Stable
- β^- 衰变 β^- decay
- β^+ 或 EC 衰变 β^+ or EC decay
- α 衰变 α decay
- 自发裂变 Spontaneous fission
- 中子发射 Neutron decay
- 质子发射 Proton decay
- 衰变类型未知 Decay mode: ?

● 已观测到、但质量未知的核素（共计809个）
 Observed nuclide with unknown mass (809)



三体核反应



Contents I

1 转移反应

- 简单历史回顾
- 转移反应的理论描述
- 转移反应理论中的问题

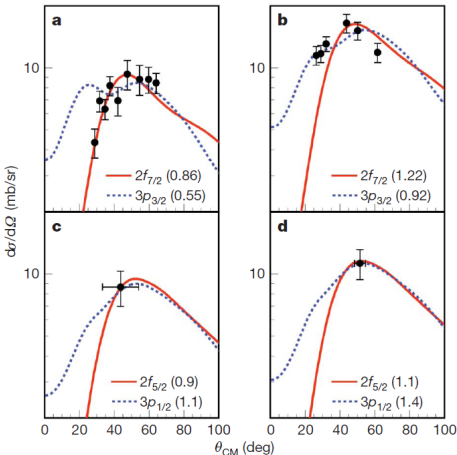
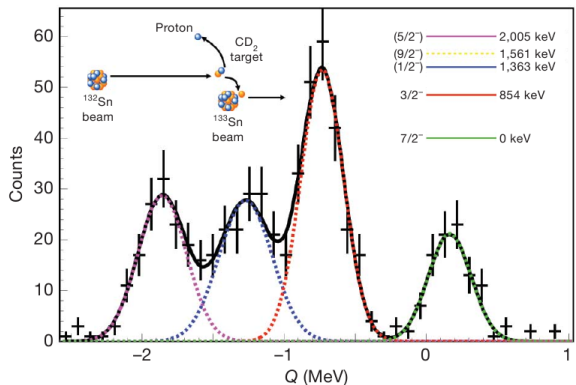
2 破裂反应

- 连续态离散化耦合道方法 (CDCC 方法)
- 弱束缚核弹性散射的破裂道耦合效应

转移反应

转移反应作为谱学工具

$d(^{132}\text{Sn}, p)^{133}\text{Sn}$ reaction at 4.77 MeV/nucleon.



K.L. Jones et al., Nature, 465, 454 (2010)

1933: possibly the first (d,p) reaction measured

The Emission of Protons from Various Targets Bombarded by Deutons of High Speed

Deutons (nuclei of H²) with energies ranging from 600,000 to 1,330,000 volts have been directed against the following targets: carbon, gold, platinum, lithium fluoride, silicon dioxide, sodium phosphate, calcium chlorate, copper sulphide and brass (the backing of the other targets). In addition to the emission of alpha-particles, which we have already reported in the preceding communication, we have observed the emission of protons in large numbers, with various ranges up to more than forty centimeters.

Every target, including gold and platinum which could hardly be expected to suffer nuclear disintegration, yielded protons of about 18 cm range in air. We have been unable to account for this group of protons common to all targets except on the hypothesis that the deuton itself is breaking up, presumably into a proton and a neutron. This assumption

ERNEST O. LAWRENCE
M. STANLEY LIVINGSTON
GILBERT N. LEWIS

Radiation Laboratory, Department of Physics,
Department of Chemistry,
University of California,
June 10, 1933.

Ernest O. Lawrence, Phys. Rev. 45, 66 (1933)

1934

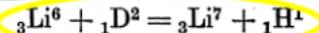
Experiments with High Velocity Positive Ions. III.—The Disintegration of Lithium, Boron, and Carbon by Heavy Hydrogen Ions.

By J. D. COCKCROFT, Ph.D., and E. T. S. WALTON, Ph.D.

(Communicated by Lord Rutherford, O.M., F.R.S.—Received April 4, 1934.)

5. *The Mechanism of the Disintegration.*

If we make the assumption that the following nuclear reaction occurs



the kinetic energy change in the transmutation may be calculated from the mass change

$$\begin{aligned} (6.0145 + 2.0136) - (7.0146 + 1.0078) \\ = 0.0057 \pm 0.0007 = 5.3 \pm 0.6 \text{ million volts.} \end{aligned}$$

1934

Experiments with High Velocity Positive Ions. III.—The Disintegration of Lithium, Boron, and Carbon by Heavy Hydrogen Ions.

By J. D. COCKCROFT, Ph.D., and E. T. S. WALTON, Ph.D.

(Communicated by Lord Rutherford, O.M., F.R.S.—Received April 4, 1934.)

5. *The Mechanism of the Disintegration.*

If we make the assumption that the following nuclear reaction occurs



the kinetic energy change in the transmutation may be calculated from the mass change

$$(6.0145 + 2.0136) - (7.0146 + 1.0078) \\ = 0.0057 \pm 0.0007 = 5.3 \pm 0.6 \text{ million volts.}$$

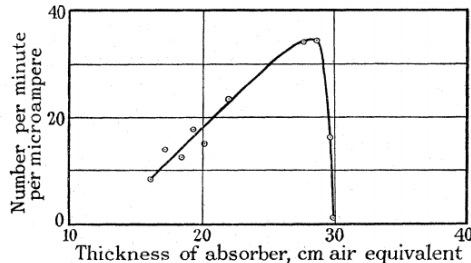


FIG. 1.—Protons from lithium.

Cockcroft and Walton, Porc. Roy. Soc. A144, 704 (1934)

1947

PHYSICAL REVIEW

VOLUME 73, NUMBER 3

FEBRUARY 1, 1948

Angular Distribution of the (d,p) Reactions Making Two Low States of O¹⁷

N. P. HEYDENBURG

Department of Terrestrial Magnetism of The Carnegie Institution of Washington, Washington, D. C.

AND

D. R. INGLIS

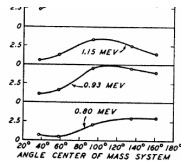
Department of Physics, The Johns Hopkins University, Baltimore, Maryland

(Received October 27, 1947)

antly as the square of one wave function, or as the superposition of the squares of several wave functions but with similar angular properties. At some higher bombarding energies no low dip in the intensity appears at any angle, and there is thus no evidence that one wave function or type of wave function predominates. Whether there be one or several components of the intensity distribution, it would be expected that it could be expressed as a sum of terms of the form

$$\sin^m \theta_r \cos^n \theta_r,$$

with the exponents m and n going to values not more than twice the highest orbital angular



SHORT RANGE GROUP, ANGULAR DISTRIBUTION OF PROTONS
 $O^{16}(d,p)O^{17}$

FIG. 5. Angular distributions of the short-range protons observed with a thin oxide target on steel.

momentum quantum number involved in the outgoing waves. With five observed values of

TABLE IV. Comparison of Observed and Calculated Angular Distributions

Heydenburg and Inglis, Phys.Rev. 73, 230 (1948).

1950：转移反应作为谱学工具的开始！

Angular Distributions of Protons from the Reaction $O^{16}(d, p)O^{17}$

HANNAH B. BURROWS
University of Liverpool, Liverpool, England
 W. M. GIBSON
University of Bristol, Bristol, England

AND
 J. ROTBLAT
Medical College of St. Bartholomew's Hospital, London, England
 October 30, 1950

We have used the 8-Mev deuteron beam from the University of Liverpool cyclotron, and a scattering camera in which photographic plates record particles emitted from a gas target at all angles from 10° to 165° , to obtain detailed angular distributions

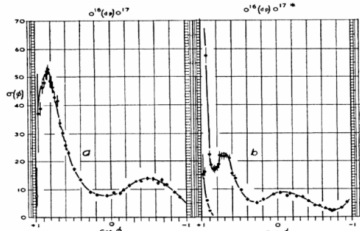


FIG. 1. $O^{16}(d, p)O^{17}$ angular distributions in the center-of-mass (c.m.) system: θ = c.m. angle, $\sigma(\theta)$ = c.m. differential cross section in arbitrary units. Curve *a* is for formation of O^{17} in the ground state, and curve *b* is for the 0.88-Mev excited state.

On Angular Distributions from (d, p) and (d, n) Nuclear Reactions

S. T. BUTLER*

*Department of Mathematical Physics, University of Birmingham,
 Birmingham, England*
 October 30, 1950

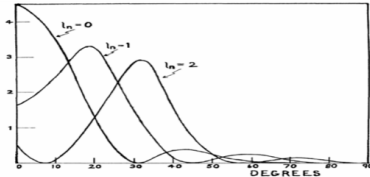


FIG. 1. Theoretical angular distributions for (d, p) and (d, n) reactions for different angular momentum transfers to the initial nucleus.

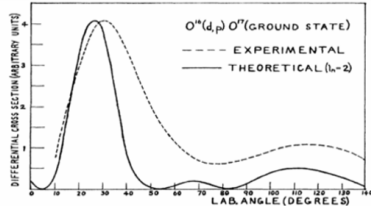


FIG. 2. Comparison of experimental and theoretical distributions for the ground-state transition of the reaction $O^{16}(d, p)O^{17}$ with 7.9-Mev incident neutrons. The theoretical curve is that for $l_n=2$.

Burrows, Gibson, Rotblat, Butler, Phys.Rev. 80, 1095 (1950)

平面波近似

$$T = \int \exp(-i\mathbf{K} \cdot \mathbf{r}) \phi_d^*(\mathbf{r}) V(\mathbf{r}) d\mathbf{r} \times \int \exp(-i\mathbf{q} \cdot \mathbf{r}_n) \phi_{nlj}(\mathbf{r}_n) d\mathbf{r}_n$$

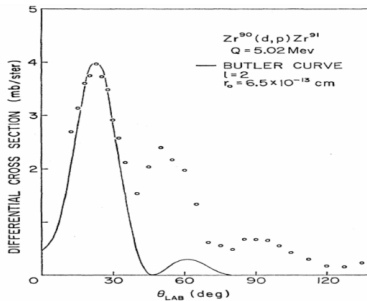


FIG. 3. The angular distribution of the proton group leading to the Zr⁹¹ ground state. The *d*-wave Butler fit agrees with the measured spin of 5/2⁺ for the state and with the shell-model expectations.

R.L.Preston et al., Phys. Rev. 121, 1741 (1961).

Cut off radius: $R = 4.37 + 0.042A$ or $1.7 + 1.22A^{1/3}$ fm for light nuclei at above Coulomb barrier.

1953：核反应机制

The Mechanism of Stripping Reactions

J. HOROWITZ AND A. M. L. MESSIAH

Centre d'Etudes Nucleaires de Saclay, Saclay, France

(Received October 8, 1953)

proton outgoing wave itself. It is more convenient to consider the matrix element $I = \langle d | N + P | \Psi \rangle$ for the time-reversed process $\mathcal{N}_2(p, d)\mathcal{N}_1$. Both matrix elements are related in a well-known fashion. Ψ is the exact wave function for a stationary state of collision $p + \mathcal{N}_2$. An approximate value for I is obtained by:

- (a) neglecting V in the Schrödinger equation for Ψ ;
- (b) replacing P everywhere by a fixed average potential Φ with the effect that Ψ becomes the product of ψ_2 by a proton plane wave plus a wave elastically scattered by potential Φ .

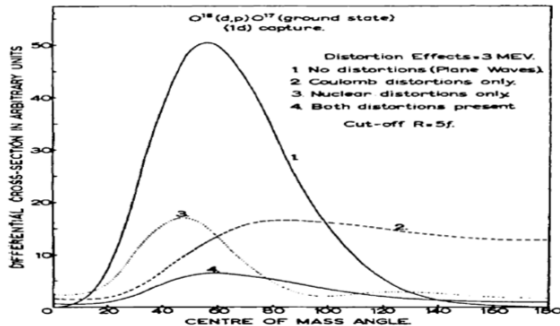
J.Horowitz and A.M.L. Messiah, Phys.Rev. 92, 1326 (1953)

1961：扭曲波波恩近似

The Analysis of (d, p) Stripping Reactions by the Distorted Wave Born Approximation

By B. BUCK† and P. E. HODGSON
Clarendon Laboratory, Oxford

[Received March 11, 1961]



B.Buck and P.E. Hodgson, Phil.Mag. 6, 1371 (1961)

1962

Volume 1, number 1

PHYSICS LETTERS

1 April 1962

made with the same target and at the same bombarding energy to measure the angular distribution of the elastically scattered deuterons. A self-supporting target of Se^{77} was then bombarded with 13.0 MeV protons and a further exposure made to measure the proton elastic scattering.

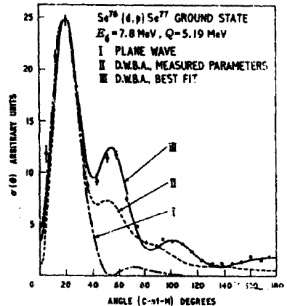
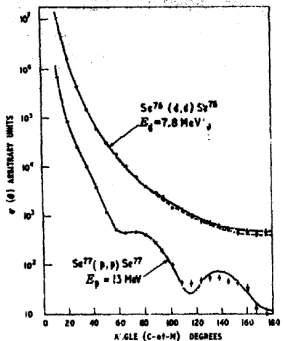


Fig. 2. Differential cross-section for the $\text{Se}^{76}(d,p)\text{Se}^{77}$ ground state proton group for $E_d = 7.8 \text{ MeV}$.

of the ground state proton group from the $\text{Se}^{76}(d,p)\text{Se}^{77}$ reaction. Curve I illustrates the best fit that could be obtained from plane-wave theory for $l = 1$. It may be noted that to fit the stripping peak successfully a radius of interaction of 5.0 fm had to be used commensurate with the Gamow-Greco-

S. Hinds and R. Middleton, Phys. Lett. 1, 12 (1962)

1963

2.F

Nuclear Physics 55 (1964) 1–33; © North-Holland Publishing Co., Amsterdam

Not to be reproduced by photoprint or microfilm without written permission from the publisher

THE DISTORTED-WAVES THEORY OF DIRECT NUCLEAR REACTIONS WITH SPIN-ORBIT EFFECTS

G. R. SATCHLER

Oak Ridge National Laboratory, Oak Ridge, Tennessee

Received 12 December 1963

Abstract: A general and flexible formulation is given of the distorted-waves theory of direct nuclear reactions which takes account of the effects of including spin-orbit coupling in the distortion, and which does not make the zero-range approximation. The evaluation of the transition amplitude is shown to involve two distinct steps, one the construction of a form factor which characterizes the particular reaction mode and the particular nuclei, and the other the treatment of the dynamics of the distorted waves, which is similar for all reactions. Expressions are given for various differential cross-sections and polarizations. As examples, procedures for treating inelastic scattering and stripping and knock-on reactions are described. The symmetry properties of the reaction amplitudes are also discussed.

G.R. Satchler, Nucl. Phys. 55, 1 (1964)

1968

2.G

Nuclear Physics A119 (1968) 241—289; © North-Holland Publishing Co., Amsterdam

Not to be reproduced by photoprint or microfilm without written permission from the publisher

**SOME STUDIES OF REALISTIC FORM FACTORS
FOR NUCLEON-TRANSFER REACTIONS**

R. J. PHILPOTT and W. T. PINKSTON

*Vanderbilt University,
Nashville, Tennessee*

and

G. R. SATCHLER
*Oak Ridge National Laboratory
Oak Ridge, Tennessee*[†]

Received 24 May 1968

Abstract: The effect of nuclear structure details on pick-up and stripping form factors is investigated. After a short review of other calculations, an approximate method is set up in which the form factor emerges as the solution of an inhomogeneous differential equation. The requirement that the derived spectroscopic amplitudes agree with corresponding shell-model amplitudes is shown to impose a condition on the potentials employed. For pick-up reactions involving the "small" components of the wave functions, structure effects often tend to enhance the form factor in the surface region. For stripping reactions, the opposite is true. The $^{60}\text{Ni}(\text{p}, \text{d})$ reaction has been studied in some detail with particular attention to the effect produced by different choices for the nuclear wave functions and residual nucleon-nucleon force. The distorted wave analysis, which mediates the comparison with experiment, is critically appraised. Although the derived angular distributions do not vary greatly, the extracted spectroscopic factors are found to be sensitive to the assumptions used. In addition, some preliminary work on the $^{40}\text{Ca}(\text{p}, \text{d})$ reaction is reported.

Problems raised to the distorted-wave method in 1968

- 1 Ambiguities and **uncertainties in optical model parameters**;
- 2 elastic parts only of the scattering wave functions may not be sufficient;
- 3 Non-locality of optical model potentials is usually neglected;
- 4 Core excitation effects to weak transitions;
- 5 D-state contributions of projectile (d , ${}^3\text{He}$, etc.);
- 6 Breakup effects of the projectile;
- 7 Elastic scattering measurements only determine the asymptotic form of the distorted waves, which are **extrapolated in the nuclear interior**;

R.J. Philpott, W.T. Pinkston and G.R. Satchler, NPA119, 241 (1968)

Transition amplitude of (d,p) reaction

Transition amplitude:

$$\begin{aligned} T_{\beta\alpha} &= \langle \chi_{pF}^{(-)} \Phi_F(\xi, \mathbf{r}_n) | V_\beta - U_\beta | \Psi_A(\xi) \phi_d(\mathbf{r}) \Psi_\alpha^{(+)} \rangle \\ &= \langle \chi_{pF}^{(-)} I_A^F | U_{pA} + V_{pn} - U_{pF} | \Psi_\alpha^{(+)} \rangle \end{aligned}$$

$$I_A^F(\mathbf{r}_n) = \sqrt{A+1} \langle \Phi_A(\xi) | \Phi_F(\xi, \mathbf{r}_n) \rangle.$$

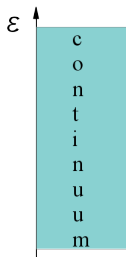
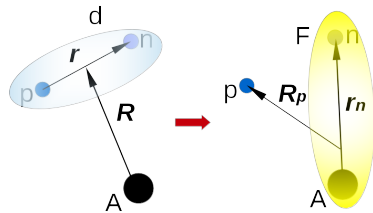
$$H\Psi_\alpha^{(+)}(\mathbf{r}, \mathbf{R}) = E\Psi_\alpha^{(+)}(\mathbf{r}, \mathbf{R}),$$

$$H = T_R + H_{np} + U_{nA} + U_{pA}$$

expand $\Psi_i^{(+)}$ with eigenfunctions of H_{np} :

$$\Psi_\alpha^{(+)}(\mathbf{r}, \mathbf{R}) = \phi_0(\mathbf{r}) \chi_0^{(+)}(\mathbf{R}) + \int dk \phi_k(\varepsilon_k, \mathbf{r}) \chi_k^{(+)}(\varepsilon_k, \mathbf{R}).$$

DWBA, ADWA, CDCC: different approximations to $\Psi_i^{(+)}$



Transition amplitude of (d,p) reaction

Transition amplitude:

$$\begin{aligned} T_{\beta\alpha} &= \langle \chi_{pF}^{(-)} \Phi_F(\xi, \mathbf{r}_n) | V_\beta - U_\beta | \Psi_A(\xi) \phi_d(\mathbf{r}) \Psi_\alpha^{(+)} \rangle \\ &= \langle \chi_{pF}^{(-)} I_A^F | U_{pA} + V_{pn} - U_{pF} | \Psi_\alpha^{(+)} \rangle \end{aligned}$$

$$I_A^F(\mathbf{r}_n) = \sqrt{A+1} \langle \Phi_A(\xi) | \Phi_F(\xi, \mathbf{r}_n) \rangle.$$

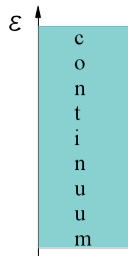
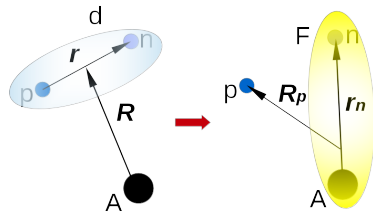
$$H\Psi_\alpha^{(+)}(\mathbf{r}, \mathbf{R}) = E\Psi_\alpha^{(+)}(\mathbf{r}, \mathbf{R}),$$

$$H = T_R + H_{np} + U_{nA} + U_{pA}$$

expand $\Psi_i^{(+)}$ with eigenfunctions of H_{np} :

$$\Psi_\alpha^{(+)}(\mathbf{r}, \mathbf{R}) = \phi_0(\mathbf{r}) \chi_0^{(+)}(\mathbf{R}) + \int dk \phi_k(\varepsilon_k, \mathbf{r}) \chi_k^{(+)}(\varepsilon_k, \mathbf{R}).$$

DWBA, ADWA, CDCC: different approximations to $\Psi_i^{(+)}$

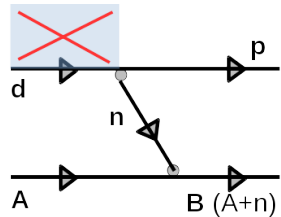


Distorted wave Born approximation: DWBA

$$\Psi_i^{(+)}(\mathbf{r}, \mathbf{R}) = \phi_0(\mathbf{r})\chi_0^{(+)}(\mathbf{R}) + \boxed{\int dk \phi_k(\varepsilon_k, \mathbf{r}) \chi_k^{(+)}(\varepsilon_k, \mathbf{R})}.$$

DWBA takes the first term of $\Psi_i^{(+)}$:

$$\begin{aligned}\Psi_i^{(+)}(\mathbf{r}, \mathbf{R}) &\simeq \phi_0(\mathbf{r})\chi_0^{(+)}(\mathbf{R}) \\ M_{fi}^{\text{DWBA}} &= \left\langle \chi_{pF}^{(-)} \psi_{nA} | \Delta V | \phi_0(\mathbf{r}) \chi_0^{(+)}(\mathbf{R}) \right\rangle.\end{aligned}$$



with DWBA:

- U_{dA} : optical model potential (describe $d + A$ **elastic scattering**)
- Assume **breakup** effect taken into account in U_{dA}
- Omit all except elastic component in the three-body wave function

Improvement: the adiabatic model: ADWA

The three-body wave function:

$$\begin{aligned} & \left[E + \varepsilon_d - \hat{T}_{cm} - U_{nA} - U_{pA} \right] \phi_d \chi_0(\mathbf{R}) \\ & + \int dk \left[E - \varepsilon_k - \hat{T}_{cm} - U_{nA} - U_{pA} \right] \phi_k(\varepsilon_k) \chi_k(\varepsilon_k, \mathbf{R}) = 0. \end{aligned}$$

Adiabatic approx.: replacing $-\varepsilon_d$ with ε_k :

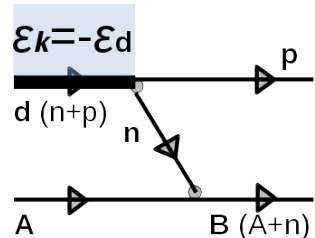
$$\left[E + \varepsilon_d - \hat{T}_{cm} - (U_{nA} + U_{pA}) \right] \tilde{\chi}_d^{ad(+)}(\mathbf{R}) = 0$$

With the adiabatic approximation:

$$M_{fi}^{\text{ADWA}} = \left\langle \chi_{pF}^{(-)} \psi_{nA} | U_{pA} + V_{pn} - U_{pF} | \phi_0(\mathbf{r}) \tilde{\chi}_d^{ad(+)} \right\rangle$$

effective $d - A$ interaction (zero-range): $U_{dA} = U_{nA} + U_{pA}$

R.C. Johnson, and P.J.R. Soper, Phys. Rev. C 1, 976 (1970).



Further Improvement: CDCC

In the CDCC method **Continuum states are Discretised into bin states**

$$\Psi_i^{(+)}(\mathbf{r}, \mathbf{R}) = \phi_0(\mathbf{r})\chi_0^{(+)}(\mathbf{R}) + \int dk \phi_k(\varepsilon_k, \mathbf{r})\chi_k^{(+)}(\varepsilon_k, \mathbf{R})$$

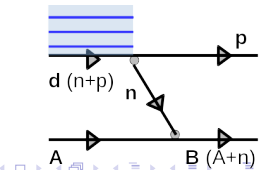
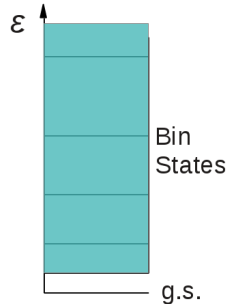
$$\Rightarrow \Psi_i^{(+)\text{CDCC}}(\mathbf{r}, \mathbf{R}) = \phi_0(\mathbf{r})\chi_0^{(+)}(\mathbf{R}) + \sum_{j=1} \phi_j^{\text{bin}}(\mathbf{r})\chi_j^{(+)}(\mathbf{R}).$$

Three-body equation turned into **Coupled-Channel equations**:

$$(T_R + H_r + U_{nA} + U_{pA}) \sum_{j=0} \phi_j(\mathbf{r})\chi_j^{(+)}(\mathbf{R}) = E \sum_{j=0} \phi_j(\mathbf{r})\chi_j^{(+)}(\mathbf{R}).$$

$$\Rightarrow (T_R + \epsilon_i - E + U_{ii})\chi_i^{(+)}(\mathbf{R}) = - \sum_{j \neq i} U_{ij}\chi_j^{(+)}(\mathbf{R})$$

$$U_{ij}(R) = \langle \phi_i(\mathbf{r}) | U_{nA} + U_{pA} | \phi_j(\mathbf{r}) \rangle.$$



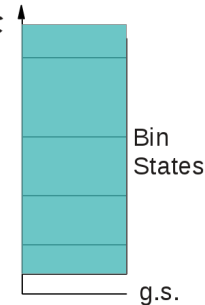
Further Improvement: CDCC

In the CDCC method **Continuum states are Discretised into bin states**

$$\Psi_i^{(+)}(\mathbf{r}, \mathbf{R}) = \phi_0(\mathbf{r})\chi_0^{(+)}(\mathbf{R}) + \int dk \phi_k(\varepsilon_k, \mathbf{r})\chi_k^{(+)}(\varepsilon_k, \mathbf{R})$$

$$\Rightarrow \Psi_i^{(+)\text{CDCC}}(\mathbf{r}, \mathbf{R}) = \phi_0(\mathbf{r})\chi_0^{(+)}(\mathbf{R}) + \sum_{j=1} \phi_j^{\text{bin}}(\mathbf{r})\chi_j^{(+)}(\mathbf{R}).$$

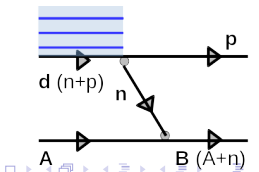
Three-body equation turned into **Coupled-Channel equations**:



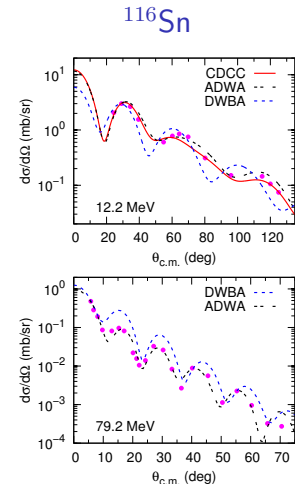
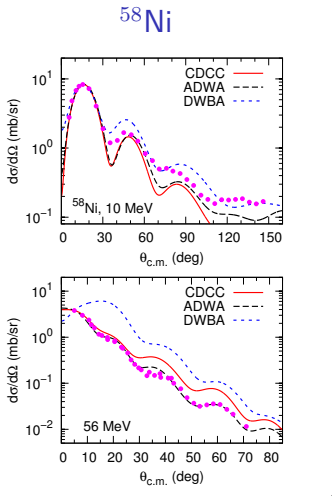
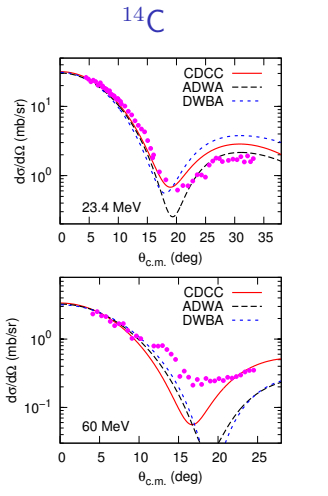
$$(T_R + H_r + U_{nA} + U_{pA}) \sum_{j=0} \phi_j(\mathbf{r})\chi_j^{(+)}(\mathbf{R}) = E \sum_{j=0} \phi_j(\mathbf{r})\chi_j^{(+)}(\mathbf{R}).$$

$$\Rightarrow (T_R + \epsilon_i - E + U_{ii})\chi_i^{(+)}(\mathbf{R}) = - \sum_{j \neq i} U_{ij}\chi_j^{(+)}(\mathbf{R})$$

$$U_{ij}(R) = \langle \phi_i(\mathbf{r}) | U_{nA} + U_{pA} | \phi_j(\mathbf{r}) \rangle.$$



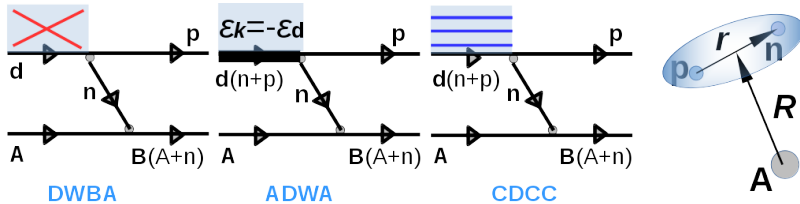
Comparisons between DWBA, ADWA, and CDCC



Pang and Mukhamedzhanov, Phys.Rev.C 90, 044611 (2014);

Mukhamedzhanov, Pang, Bertulani, and Kadyrov, Phys.Rev.C 90, 034604 (2014)

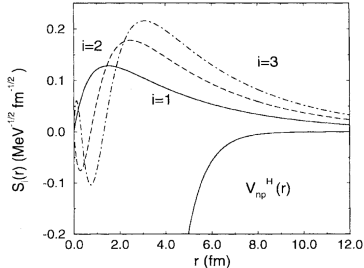
The Weinberg state expansion method



Expend the three-body wave function with
Weinberg states:

$$\Psi_i(\mathbf{r}, \mathbf{R})^{(+)} = \sum_i \phi_i^W(\mathbf{r}) \chi_i^W(\mathbf{R})$$

$$[-\varepsilon_d - T_r - \alpha_i V_{np}] \phi_i^W = 0, \quad i = 1, 2, \dots$$

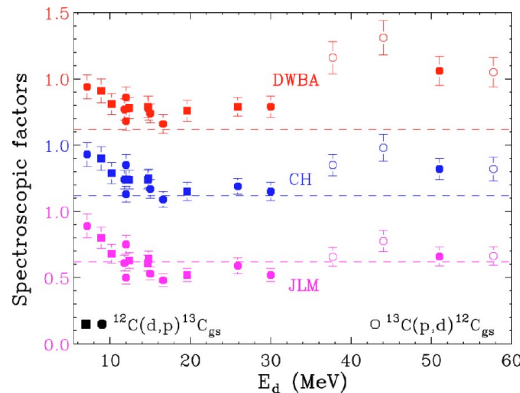
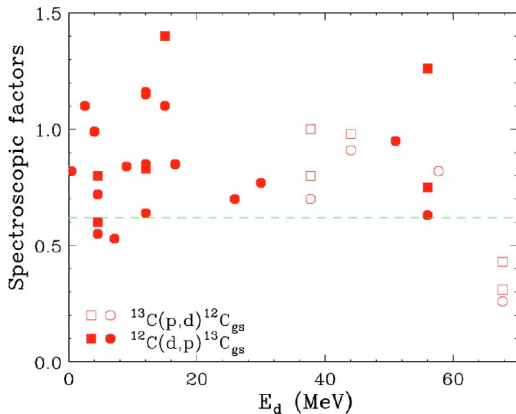


Pang, Timofeyuk, Johnson, and Tostevin, Phys. Rev. C 87, 064613 (2013).

R.C. Johnson, J. Phys. G: Nucl. Part. Phys. 41, 094005 (2014).

问题 1：应该用什么样的光学势？

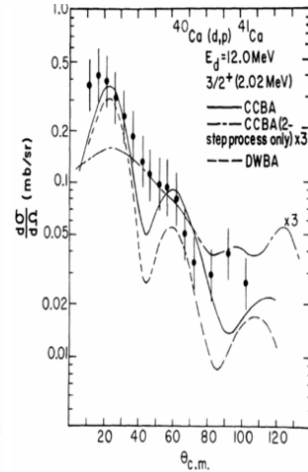
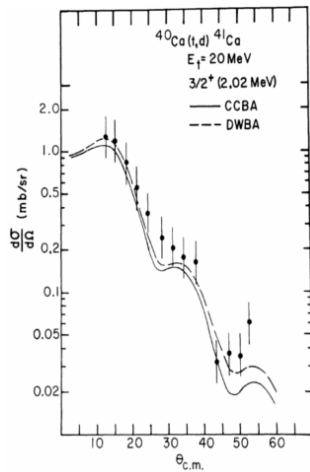
Solution: make use of systematic optical model potentials:



X.D. Liu et al., PRC 69, 064313 (2004)

问题 2：耦合道的影响

Solution: coupled channel calculations: CCBA, CRC



T. Tamura and T. Udagawa, PRC 5, 1127 (1972)

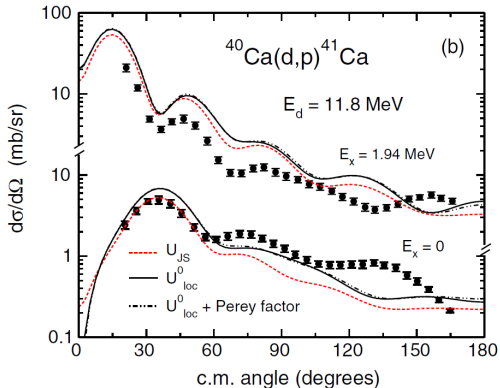
问题 3：光学势的非定域性

$$\begin{aligned} & \frac{\hbar^2}{2\mu} \left[\frac{d^2}{dr^2} - \frac{l(l+1)}{r^2} \right] u_{jl}(r) \\ & + [E - V_C(r) - (\mathbf{I}_n \cdot \mathbf{l}) V_{so}(r)] u_{jl}(r) \\ & - \int_0^\infty g_l(r, r') u_{jl}(r') dr' = 0, \end{aligned} \quad (11)$$

where [22]

$$g_l(r, r') = \frac{1}{\sqrt{\pi}\beta} \exp \left[-\left(\frac{r^2 + r'^2}{\beta^2} \right) \right] 2i^l z j_l(-iz) W(p), \quad (12)$$

and $W(p) = V_{NL} f_0(p)$, $p = \frac{r+r'}{2}$, and $z = \frac{2rr'}{\beta^2}$. Here β is the range of nonlocality and $j_l(-iz)$ is the spherical Bessel functions of the l th order.



Tianyuan, PDY and Z.Y. Ma, PRC (2018); N.K. Timofeyuk and R.C. Johnson, PRL (2013); S.J. Waldecker and N.K. Timofeyuk, PRC 94, 034609(2016)

问题 4：核心激发

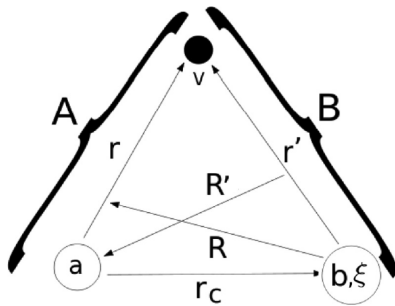
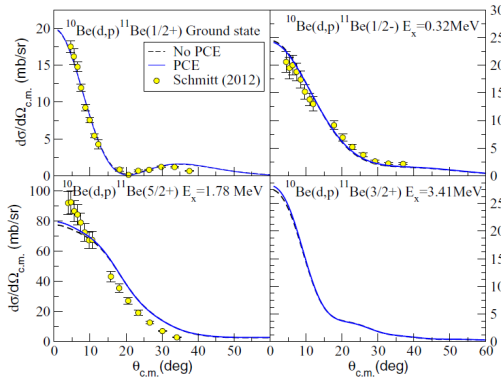


FIG. 1. Relevant coordinates involved in the calculation. a and b are the cores to which the valence particle v is bound before and after the transfer reaction.



M. Gomez-Ramos, A.M. Moro, et al., PRC (2016)

问题 5：氘核的 D 波成分

S-state dominates at low energies. Both S- and D-states are important at high energies.

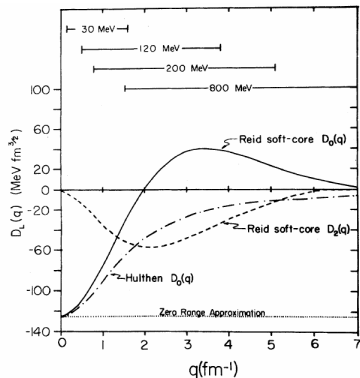


FIG. 9. The projectile Fourier transform of $V_{pn}\phi_d$ [See Eq. (4)] is shown for Hulthén and Reid soft-core deuteron wave functions. The effective D_0 implied by the zero-range approximation is indicated by the dotted line. The horizontal bars show the range of momentum sampled by the $^{12}\text{C}(\text{p},\text{d})^{11}\text{C}(\text{g.s.})$ reaction at various energies assuming no distortion effects (PWBA).

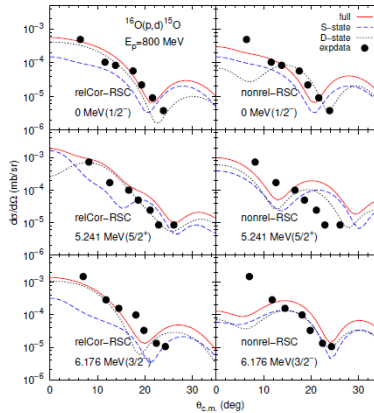


图 29 以 $^{16}\text{O}(p, d)^{15}\text{O}$, $E_p = 800$ MeV 的结果为例, 展示氘核 S 态和 D 态分别对转移反应截面的贡献。实线、虚线和点线分别对应包含全部态, 只考虑氘核 S 态贡献和只考虑氘核 D 态的结果, 实心圆点表示实验数据。图中(左)(右)两列分别对应考虑相对论修正和不考虑相对论修正的数据。计算中所使用的核波函数为 Reid soft-core。

问题 6：弹核破裂反应的影响

Solutions: Adiabatic model (ADWA), CDCC, etc.

PHYSICAL REVIEW C

VOLUME 1, NUMBER 3

MARCH 1970

Contribution of Deuteron Breakup Channels to Deuteron Stripping and Elastic Scattering

R. C. JOHNSON

Department of Physics, University of Surrey, Guildford, Surrey, England

AND

P. J. R. SOPER*

International Centre for Theoretical Physics, Trieste, Italy

(Received 10 November 1969)

We present a model of deuteron stripping and elastic scattering which treats explicitly the contributions from channels in which the deuteron is broken up into a relative S state and the target is in its ground state. An adiabatic treatment of these channels leads to a description of deuteron stripping which resembles the distorted-wave Born approximation, although a deuteron optical potential plays no role. The adiabatic approximation is shown to give a good account of 21.6-MeV elastic deuteron scattering from Ni, at least for surface partial waves, and is expected to apply to other nuclei in this mass and energy region, as well as at higher energies. The calculations assume that the effective two-nucleon–nucleus interaction is the sum of the nucleon optical potentials evaluated at one-half the incident deuteron kinetic energy. Some possible corrections to this assumption are discussed.

问题 7：散射波的内部波函数

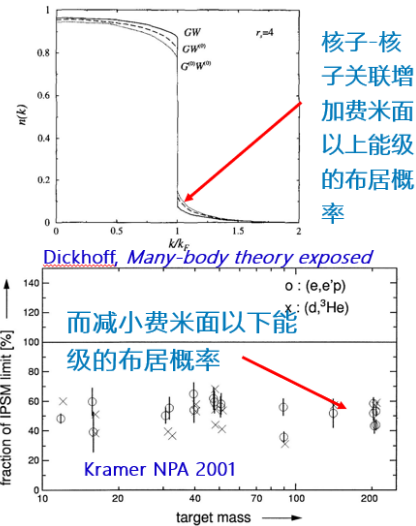
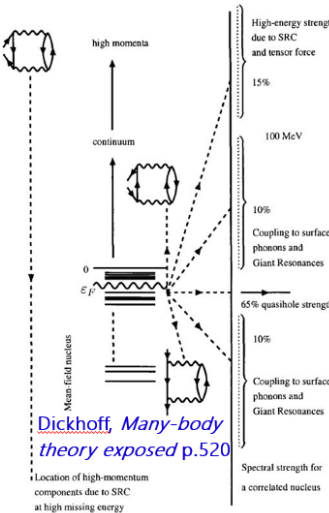
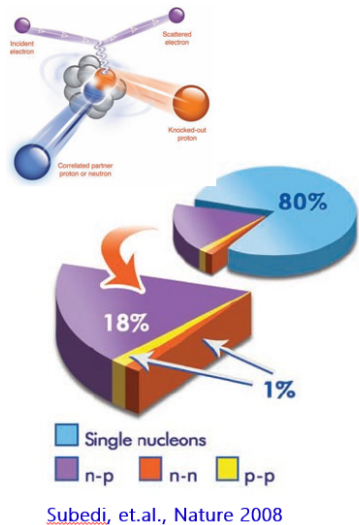
Solution???: make use of systematic **microscopic** optical model potentials:

Table 1 Single particle orbitals of transferred neutrons (nlj), r_0 values of single particle potentials, and incident energies (E_{lab}) for the three reactions. The reduction factors of single particle strength (R_s) are obtained as ratios of experimental and theoretical (shell model) SFs, SF^{exp} and SF^{SM} , respectively. $\langle R_s \rangle$ are the averaged values of R_s evaluated at the two incident energies for each reaction. CH89 and CTOM are analyzed. A unified uncertainty of 26% is applied to the SF^{exp} and R_s values. See the text for details

Target	nlj	r_0 (fm)	SF^{SM}	E_{lab} (MeV)	SF^{exp}	R_s	$\langle R_s \rangle$	SF^{exp}	R_s	$\langle R_s \rangle$
					CH89			CTOM		
^{14}C	$2s_{1/2}$	1.273	1.107	14	1.11 ± 0.26	1.00 ± 0.26	0.87 ± 0.23	0.75 ± 0.20	0.67 ± 0.17	0.62 ± 0.16
				60	0.83 ± 0.22	0.75 ± 0.20		0.62 ± 0.16	0.56 ± 0.15	
^{36}S	$1f_{7/2}$	1.220	0.980	12.3	0.79 ± 0.21	0.81 ± 0.21	0.81 ± 0.21	0.70 ± 0.18	0.72 ± 0.19	0.70 ± 0.18
				25	0.79 ± 0.21	0.81 ± 0.21		0.67 ± 0.17	0.68 ± 0.18	
^{58}Ni	$2p_{3/2}$	1.154	0.572	10	0.53 ± 0.14	0.92 ± 0.24	1.04 ± 0.27	0.38 ± 0.10	0.66 ± 0.17	0.69 ± 0.18
				56	0.66 ± 0.17	1.15 ± 0.30		0.41 ± 0.11	0.72 ± 0.19	

Yun Xiaoyan, PDY, et al., SCPMA, (2020)

补充说明：原子核中的核子-核子关联



谱因子和渐进归一化系数

- The deuteron stripping amplitude:

$$T = \langle \chi_{pF}^{(-)} \Phi_F(\xi_A, \mathbf{r}_n) | U_{pA} + V_{pn} - U_{pF} | \Phi_A(\xi_A) \phi_d(\mathbf{r}) \Psi_i^{(+)} \rangle$$

- The overlap function I_A^F :

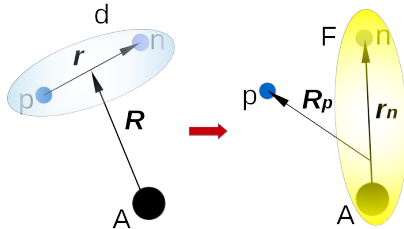
$$I_A^F(\mathbf{r}_n) = \sqrt{A+1} \langle \Phi_A(\xi_A) | \Phi_F(\xi_A, \mathbf{r}_n) \rangle.$$

- Parentage expansion:

$$\Phi_F^{J_F, M_F}(\mathbf{A}, \mathbf{r}_n) = \sum_{\mathbf{A}', j\ell} \beta_{j\ell}(B, A') \mathcal{A} [\Phi_{J_{A'}} \psi_{n\ell j}(\mathbf{r}_n)]_{J_F}^{M_F}$$

- The deuteron stripping amplitude:

$$T = I_A^F \langle \chi_{pF}^{(-)} \psi_{n\ell j}(\mathbf{r}_n) | U_{pA} + V_{pn} - U_{pF} | \phi_d(\mathbf{r}) \Psi_i^{(+)} \rangle, \frac{d\sigma}{d\Omega} \propto |T|^2 \propto (I_A^F)^2 (= SF)$$



Asymptotic behaviors

- of the overlap function (ANC):

$$I_{A(\ell_{nA}j_{nA})}^F(r_{nA}) \xrightarrow{r_{nA} > R_{nA}} C_{\ell_{nA}j_{nA}} i\kappa_{nA} h_{\ell_{nA}}^{(1)}(i\kappa_{nA} r_{nA})$$

- of the neutron s.p. w.f. of $F = n + A$ (SPANC):

$$\psi_{nA(n_r\ell_{nA}j_{nA})}(r_{nA}) \xrightarrow{r_{nA} > R_{nA}} b_{n_r\ell_{nA}j_{nA}} i\kappa_{nA} h_{\ell_{nA}}^{(1)}(i\kappa_{nA} r_{nA})$$

- Asymptotically: $I_{A(\ell_{nA}j_{nA})}^F$ proportional to $\psi_{nA(n_r\ell_{nA}j_{nA})}$:

$$I_{A(\ell_{nA}j_{nA})}^F(r_{nA}) \xrightarrow{r_{nA} \geq R_{nA}} \frac{C_{\ell_{nA}j_{nA}}}{b_{n_r\ell_{nA}j_{nA}}} \psi_{nA(n_r\ell_{nA}j_{nA})}(r_{nA})$$

- **A big assumption:** such proportionality extend to all r_{nA} :

$$I_{A(\ell_{nA}j_{nA})}^F(r_{nA}) = \frac{C_{\ell_{nA}j_{nA}}}{b_{n_r\ell_{nA}j_{nA}}} \psi_{nA}(r_{nA}) \Rightarrow SF_{n_r\ell_{nA}j_{nA}} = \frac{C_{\ell_{nA}j_{nA}}^2}{b_{n_r\ell_{nA}j_{nA}}^2}$$

Asymptotic behaviors

- of the overlap function (**ANC**):

$$I_{A(\ell_{nA}j_{nA})}^F(r_{nA}) \xrightarrow{r_{nA} > R_{nA}} C_{\ell_{nA}j_{nA}} i\kappa_{nA} h_{\ell_{nA}}^{(1)}(i\kappa_{nA} r_{nA})$$

- of the neutron s.p. w.f. of $F = n + A$ (**SPANC**):

$$\psi_{nA(n_r\ell_{nA}j_{nA})}(r_{nA}) \xrightarrow{r_{nA} > R_{nA}} b_{n_r\ell_{nA}j_{nA}} i\kappa_{nA} h_{\ell_{nA}}^{(1)}(i\kappa_{nA} r_{nA})$$

- Asymptotically: $I_{A(\ell_{nA}j_{nA})}^F$ proportional to $\psi_{nA(n_r\ell_{nA}j_{nA})}$:

$$I_{A(\ell_{nA}j_{nA})}^F(r_{nA}) \xrightarrow{r_{nA} \geq R_{nA}} \frac{C_{\ell_{nA}j_{nA}}}{b_{n_r\ell_{nA}j_{nA}}} \psi_{nA(n_r\ell_{nA}j_{nA})}(r_{nA})$$

- **A big assumption:** such proportionality extend to all r_{nA} :

$$I_{A(\ell_{nA}j_{nA})}^F(r_{nA}) = \frac{C_{\ell_{nA}j_{nA}}}{b_{n_r\ell_{nA}j_{nA}}} \psi_{nA}(r_{nA}) \Rightarrow SF_{n_r\ell_{nA}j_{nA}} = \frac{C_{\ell_{nA}j_{nA}}^2}{b_{n_r\ell_{nA}j_{nA}}^2}$$

Asymptotic behaviors

- of the overlap function (**ANC**):

$$I_{A(\ell_{nA}j_{nA})}^F(r_{nA}) \xrightarrow{r_{nA} > R_{nA}} C_{\ell_{nA}j_{nA}} i\kappa_{nA} h_{\ell_{nA}}^{(1)}(i\kappa_{nA} r_{nA})$$

- of the neutron s.p. w.f. of $F = n + A$ (**SPANC**):

$$\psi_{nA(n_r\ell_{nA}j_{nA})}(r_{nA}) \xrightarrow{r_{nA} > R_{nA}} b_{n_r\ell_{nA}j_{nA}} i\kappa_{nA} h_{\ell_{nA}}^{(1)}(i\kappa_{nA} r_{nA})$$

- Asymptotically: $I_{A(\ell_{nA}j_{nA})}^F$ proportional to $\psi_{nA(n_r\ell_{nA}j_{nA})}$:

$$I_{A(\ell_{nA}j_{nA})}^F(r_{nA}) \xrightarrow{r_{nA} \geq R_{nA}} \frac{C_{\ell_{nA}j_{nA}}}{b_{n_r\ell_{nA}j_{nA}}} \psi_{nA(n_r\ell_{nA}j_{nA})}(r_{nA})$$

- **A big assumption:** such proportionality extend to all r_{nA} :

$$I_{A(\ell_{nA}j_{nA})}^F(r_{nA}) = \frac{C_{\ell_{nA}j_{nA}}}{b_{n_r\ell_{nA}j_{nA}}} \psi_{nA}(r_{nA}) \Rightarrow SF_{n_r\ell_{nA}j_{nA}} = \frac{C_{\ell_{nA}j_{nA}}^2}{b_{n_r\ell_{nA}j_{nA}}^2}$$

Asymptotic behaviors

- of the overlap function (**ANC**):

$$I_{A(\ell_{nA}j_{nA})}^F(r_{nA}) \xrightarrow{r_{nA} > R_{nA}} C_{\ell_{nA}j_{nA}} i\kappa_{nA} h_{\ell_{nA}}^{(1)}(i\kappa_{nA} r_{nA})$$

- of the neutron s.p. w.f. of $F = n + A$ (**SPANC**):

$$\psi_{nA(n_r\ell_{nA}j_{nA})}(r_{nA}) \xrightarrow{r_{nA} > R_{nA}} b_{n_r\ell_{nA}j_{nA}} i\kappa_{nA} h_{\ell_{nA}}^{(1)}(i\kappa_{nA} r_{nA})$$

- Asymptotically: $I_{A(\ell_{nA}j_{nA})}^F$ proportional to $\psi_{nA(n_r\ell_{nA}j_{nA})}$:

$$I_{A(\ell_{nA}j_{nA})}^F(r_{nA}) \xrightarrow{r_{nA} \geq R_{nA}} \frac{C_{\ell_{nA}j_{nA}}}{b_{n_r\ell_{nA}j_{nA}}} \psi_{nA(n_r\ell_{nA}j_{nA})}(r_{nA})$$

- **A big assumption:** such proportionality extend to all r_{nA} :

$$I_{A(\ell_{nA}j_{nA})}^F(r_{nA}) = \frac{C_{\ell_{nA}j_{nA}}}{b_{n_r\ell_{nA}j_{nA}}} \psi_{nA}(r_{nA}) \Rightarrow \boxed{SF_{n_r\ell_{nA}j_{nA}} = \frac{C_{\ell_{nA}j_{nA}}^2}{b_{n_r\ell_{nA}j_{nA}}^2}}$$

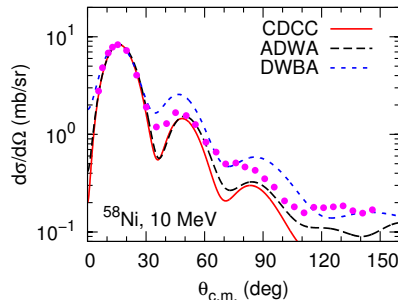
Extraction of SF and ANC from experimental data

spectroscopic factor in transition amplitude:

$$T = SF_{n_r \ell_n A j_{nA}}^{1/2} \langle \chi_{pF}^{(-)} \psi_{nA(n_r \ell_n A j_{nA})} | U_{pA} + V_{pn} - U_{pF} | \Phi_i^{(+)} \rangle.$$

Experimentally, $SF_{n_r \ell_n A j_{nA}}$ and $C_{\ell_n A j_{nA}}$ are obtained by

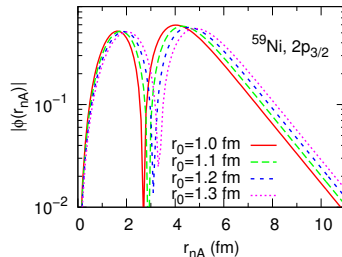
$$SF_{n_r \ell_n A j_{nA}} = \frac{d\sigma^{\text{exp}}/d\Omega}{d\sigma^{\text{th}}/d\Omega} \Rightarrow C_{\ell_n A j_{nA}}^2 = SF_{n_r \ell_n A j_{nA}} b_{n_r \ell_n A j_{nA}}^2$$



Single-particle potential for $\psi_{nA(n_r \ell_{nA} j_{nA})}$

$\psi_{nA(n_r \ell_{nA} j_{nA})}$ obtained with a Woods-Saxon potential:

$$V(r, r_0, a_0) = \frac{V_0}{1 + \exp [(r - r_0 A^{1/3})/a_0]}$$



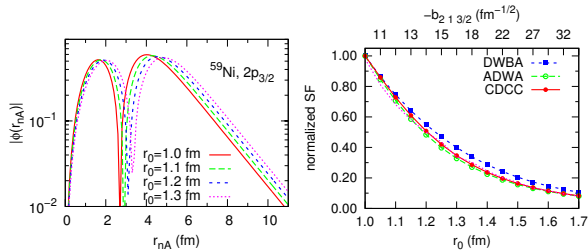
assymptotically:

$$\psi_{nA(n_r \ell_{nA} j_{nA})}(r_{nA}) \xrightarrow{r_{nA} > R_{nA}} b_{n_r \ell_{nA} j_{nA}} i \kappa_{nA} h_{\ell_{nA}}^{(1)}(i \kappa_{nA} r_{nA})$$

Single-particle potential for $\psi_{nA(n_r \ell_{nA} j_{nA})}$

$\psi_{nA(n_r \ell_{nA} j_{nA})}$ obtained with a Woods-Saxon potential:

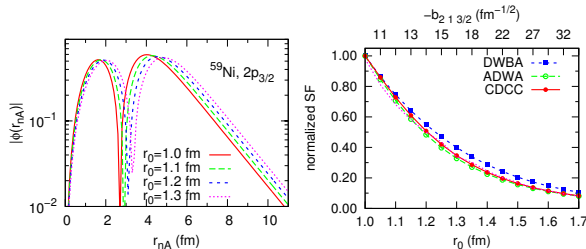
$$V(r, r_0, a_0) = \frac{V_0}{1 + \exp [(r - r_0 A^{1/3})/a_0]}$$



Single-particle potential for $\psi_{nA(n_r\ell_{nA}j_{nA})}$

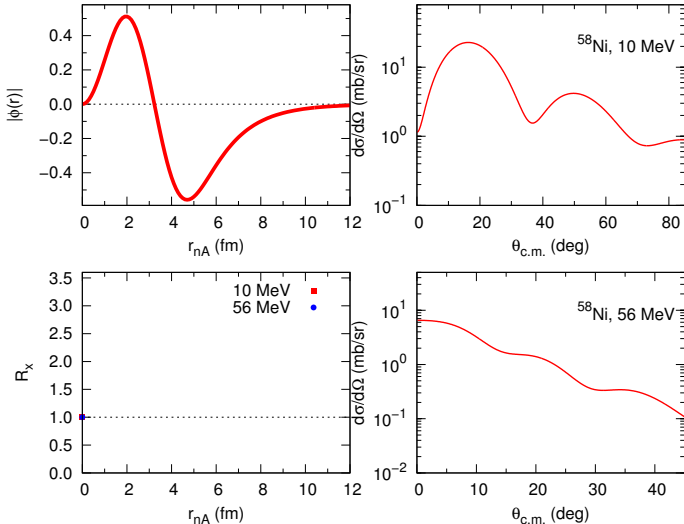
$\psi_{nA(n_r\ell_{nA}j_{nA})}$ obtained with a Woods-Saxon potential:

$$V(r, r_0, a_0) = \frac{V_0}{1 + \exp [(r - r_0 A^{1/3})/a_0]}$$

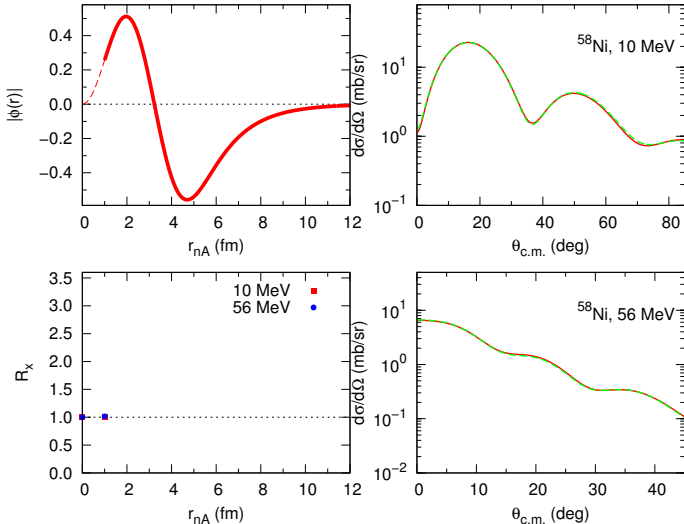


$$T = SF_{n_r\ell_{nA}j_{nA}}^{1/2} \langle \chi_{pF}^{(-)} \psi_{nA} | \Delta V_{pF} | \Phi_i^{(+)} \rangle, \quad C^2 = SF \times b^2$$

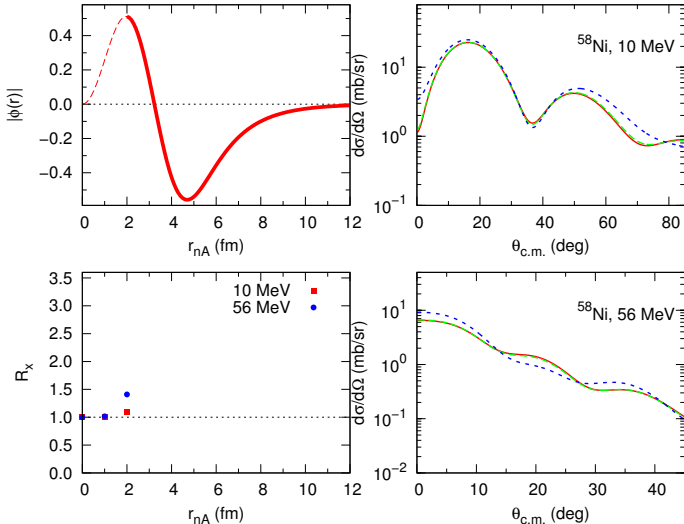
周边性检验



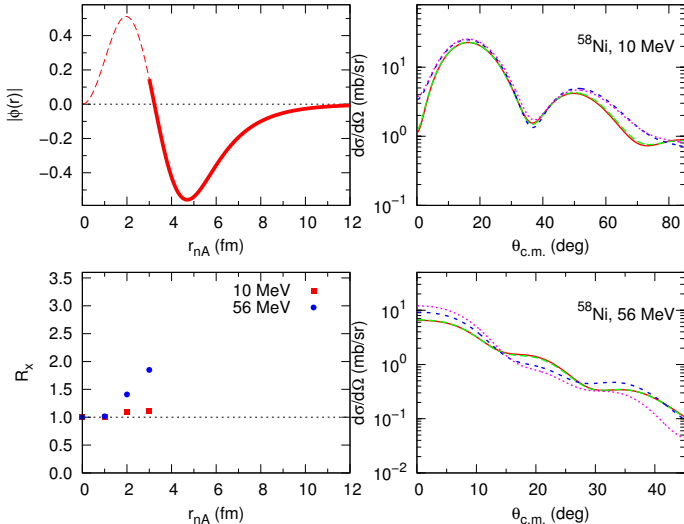
周边性检验



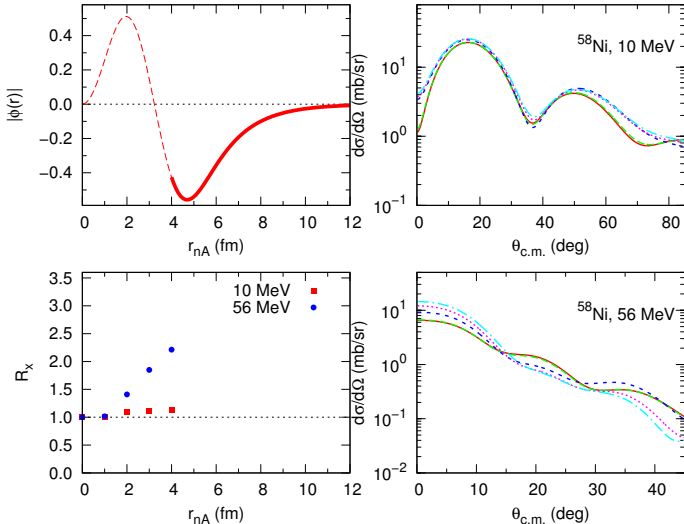
周边性检验



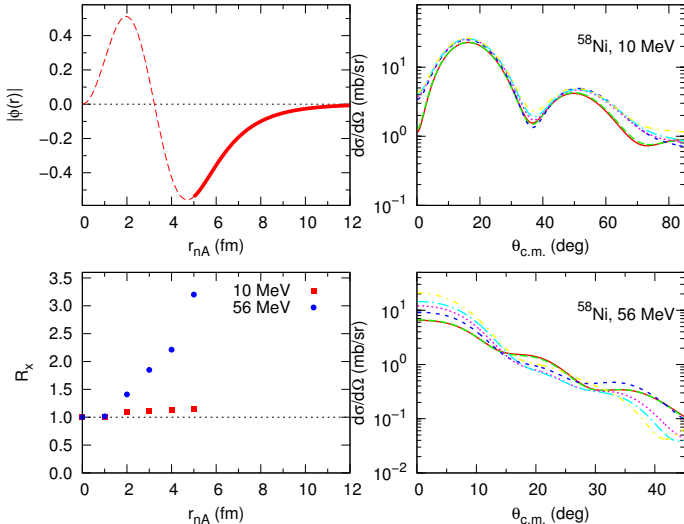
周边性检验



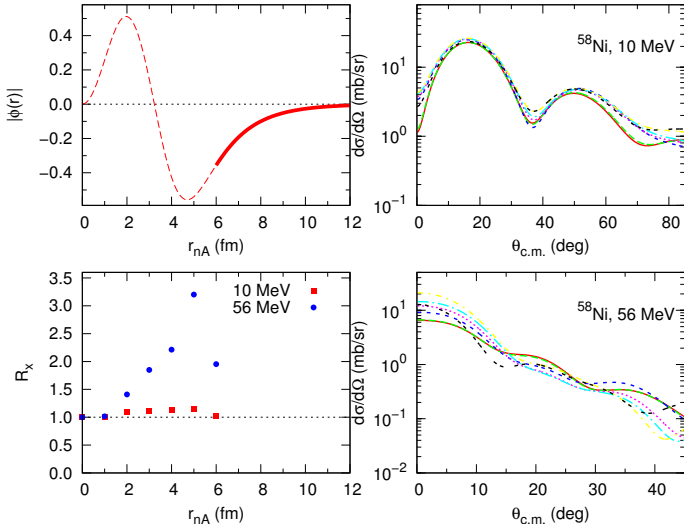
周边性检验



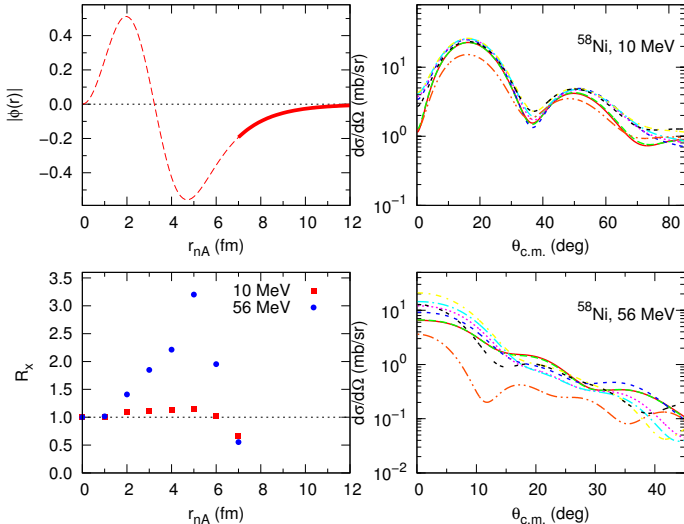
周边性检验



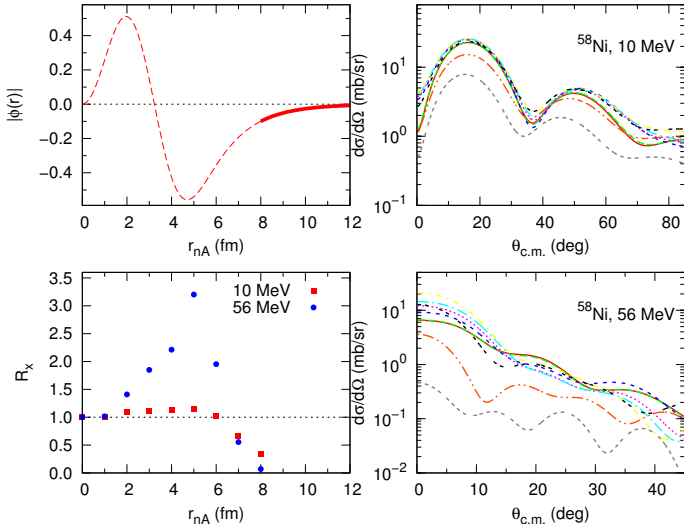
周边性检验



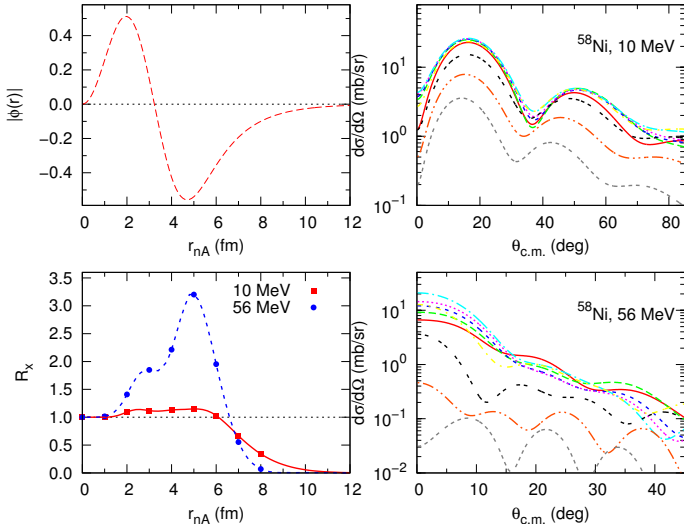
周边性检验

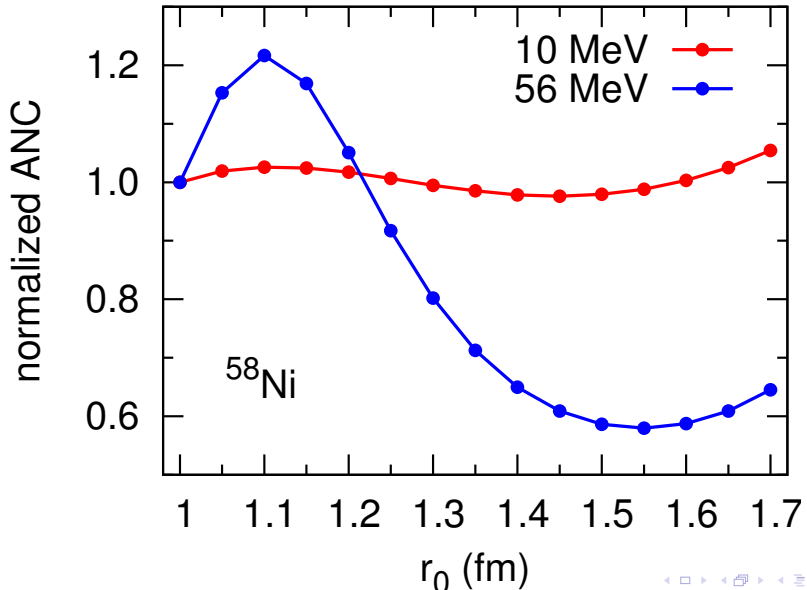


周边性检验



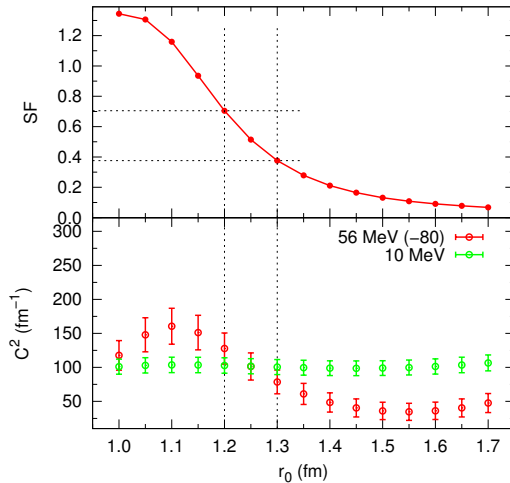
周边性检验



peripherality shown by ANC: the ^{58}Ni case

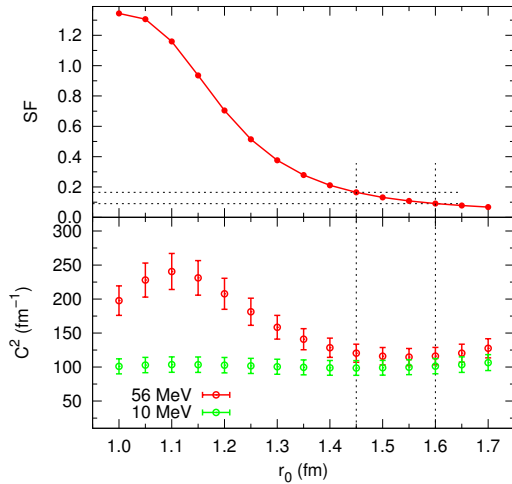
Application of the Combined method: ideally ...

For the $^{58}\text{Ni}(\text{d},\text{p})^{59}\text{Ni}$ reaction:



Application of the Combined method: actually ...

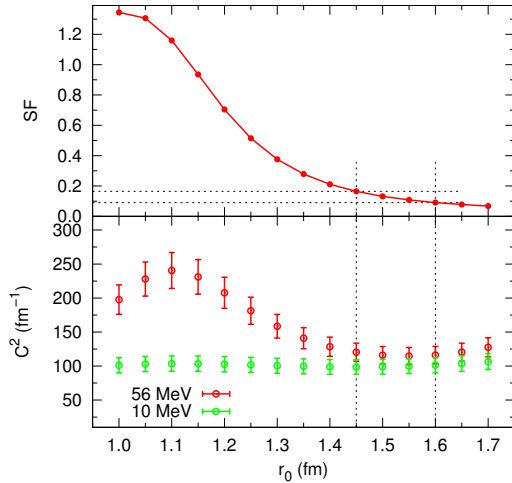
For the $^{58}\text{Ni}(\text{d},\text{p})^{59}\text{Ni}$ reaction:



The internal part of the overlap is not well represented by the single-particle wave

Application of the Combined method: actually ...

For the $^{58}\text{Ni}(\text{d},\text{p})^{59}\text{Ni}$ reaction:



The internal part of the overlap is not well represented by the single-particle wave

Need for accurate overlap functions!

- ① When SF and ANC are not compatible, the inner part of the overlap function is not represented well with the well-depth prescription;
- ② To obtain reliable SFs, improvement of the treatment of *the internal region* is necessary.

Inconsistency in neutron potentials V_{nA} and U_{nA}

$$T_{fi}^{\text{ADWA}} = \left\langle \chi_{pF}^{(-)} \psi_{nA} | U_{pA} + V_{pn} - U_{pF} | \phi_0(\mathbf{r}) \tilde{\chi}_d^{\text{ad}(+)} \right\rangle$$

- Distorted waves $\tilde{\chi}_d^{\text{ad}(+)}$ \Leftarrow complex U_{nA} $\Leftarrow \frac{d\sigma_{\text{el}}}{d\Omega}$
- Single particle wave function ψ_{nA} \Leftarrow real V_{nA} $\Leftarrow E_{\text{binding}}$

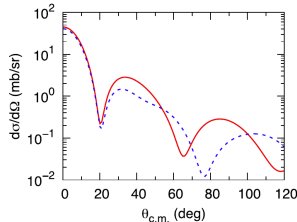


FIG. 1. (Color online) Prior DWBA differential cross sections for the $^{14}\text{C}(d, p)^{15}\text{C}$ ($2s_{1/2}, E_x = 0.0$ MeV) at $E_d = 23.4$ MeV. The solid red line is obtained using the optical potential U_{nA} when calculating U_{dA} ; the blue dotted line is obtained with $U_{nA} = V_{nA}^{\text{op}}$ in U_{dA} .

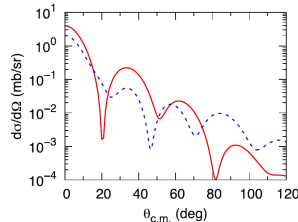


FIG. 3. (Color online) Prior DWBA differential cross sections for the $^{14}\text{C}(d, p)^{15}\text{C}$ ($2s_{1/2}, E_x = 0.0$ MeV) at $E_d = 60$ MeV. Notations are the same as in Fig. 1.

A.M. Mukhamedzhanov, DYP, C. Bertulani, A.S. Kadyrov, PRC 90, 034604 (2014)

possible solution: dispersive optical model potentials

Inconsistency in neutron potentials V_{nA} and U_{nA}

$$T_{fi}^{\text{ADWA}} = \left\langle \chi_{pF}^{(-)} \psi_{nA} | U_{pA} + V_{pn} - U_{pF} | \phi_0(\mathbf{r}) \tilde{\chi}_d^{\text{ad}(+)} \right\rangle$$

- Distorted waves $\tilde{\chi}_d^{\text{ad}(+)}$ \Leftarrow complex U_{nA} $\Leftarrow \frac{d\sigma_{\text{el}}}{d\Omega}$
- Single particle wave function ψ_{nA} \Leftarrow real V_{nA} $\Leftarrow E_{\text{binding}}$

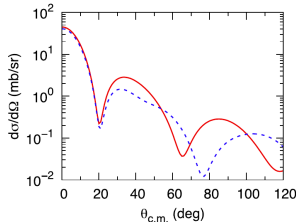


FIG. 1. (Color online) Prior DWBA differential cross sections for the $^{14}\text{C}(d, p)^{15}\text{C}(2s_{1/2}, E_d = 0.0 \text{ MeV})$ at $E_d = 23.4 \text{ MeV}$. The solid red line is obtained using the optical potential U_{nA} when calculating U_{dA} ; the blue dotted line is obtained with $U_{nA} = V_{nA}^{\text{op}}$ in U_{dA} .

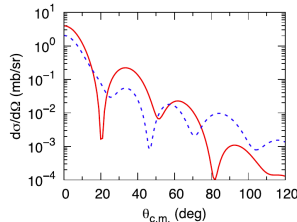


FIG. 3. (Color online) Prior DWBA differential cross sections for the $^{14}\text{C}(d, p)^{15}\text{C}(2s_{1/2}, E_d = 0.0 \text{ MeV})$ at $E_d = 60 \text{ MeV}$. Notations are the same as in Fig. 1.

A.M. Mukhamedzhanov, DYP, C. Bertulani, A.S. Kadyrov, PRC 90, 034604 (2014)

possible solution: dispersive optical model potentials

Necessity of closed channels: at year 1987

The coupled-equations method also contains “closed channels”, in which the relative energy is greater than the total energy, $\varepsilon(k) = (\hbar^2 k^2 / M) > E$, so that the associated center-of-mass functions $g_{IL}^j(\lambda, R)$ are exponentially damped asymptotically. These closed channels couple strongly to the open channels that do contain outgoing flux and they affect their properties, especially at low bombarding energies. Figure 25 shows that closed channels can make large contributions to the stripping cross section.

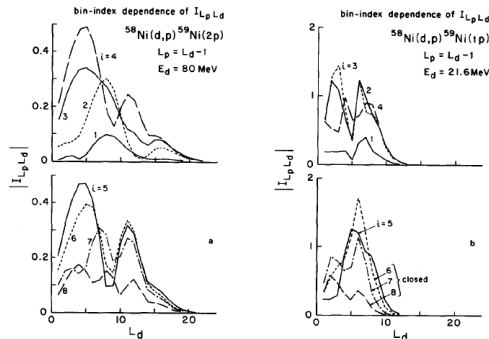


Fig. 25. Contributions to the breakup part of $I_{L_p L_d}$ from individual continuum momentum bins, for the reaction $^{58}\text{Ni}(d, p)^{59}\text{Ni}(2p, \text{g.s.})$ at (a) $E_d = 80 \text{ MeV}$ and (b) $E_d = 21.6 \text{ MeV}$. Quoted from [Is85b].

N. Austern et al.,
Phys.Rep. 154, 125 (1987)

破裂反应

连续态离散化耦合道方程

The coupled equation:

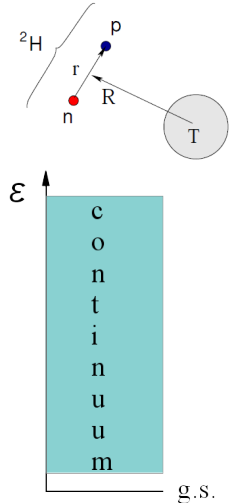
$$\Psi_{\text{model}}(\mathbf{R}, \xi) = \phi_0(\xi)\chi_0(\mathbf{K}_0, \mathbf{R}) + \sum_{n>0} \phi_n(\xi)\chi_n(\mathbf{K}_n, \mathbf{R})$$

Problems:

- There are infinite number of continuum states
- The continuum states are non-normalizable

$$\langle \phi_{k,l,sj}(r) | \phi_{k',l,sj}(r) \rangle \propto \delta(k - k')$$

- SOLUTION \Rightarrow continuum discretization

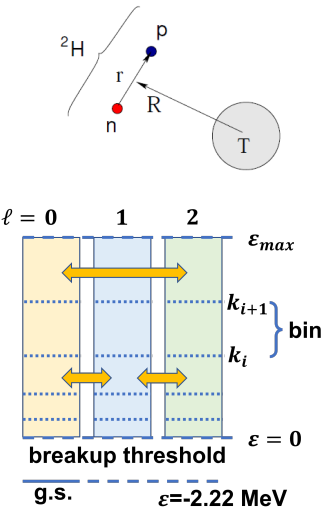


Construction of the continuum bins

- Select a number of angular momenta ($\ell = 0, 1, \dots, l_{\max}$)
- For each ℓ , set a maximum excitation energy ε_{\max}
- Divide the intervals $\varepsilon = 0 - \varepsilon_{\max}$ into a set of sub-intervals (bins)
- For each bin, calculate a representation wave function

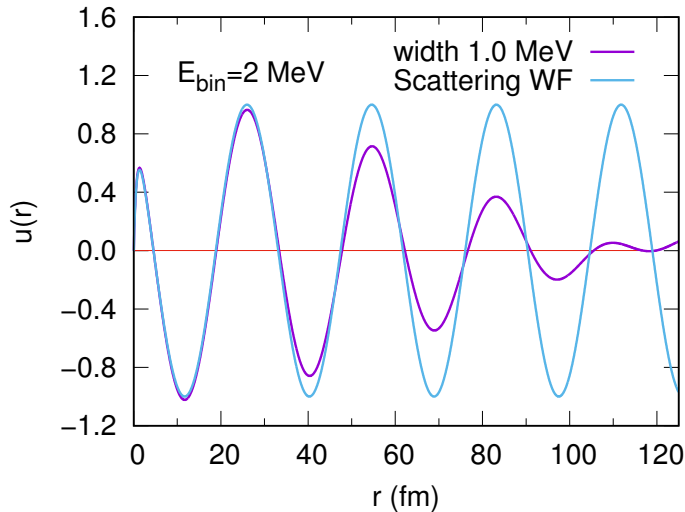
$$\phi_{\ell s j, i}^{[k_i, k_{i+1}]}(r) = \sqrt{\frac{2}{\pi N}} \int_{k_i}^{k_{i+1}} w(k) u_{k, \ell s j}(r) dk$$

- $u_{k, \ell s j}(r)$: radial scattering wave function
- $k_i = \sqrt{2\mu\varepsilon_i}/\hbar$
- $w(k)$: weight function



Construction of the continuum bins: example

deuteron ($n-p$ system) with Huthén potential, S state.



The CDCC method

- The three-body wave function:

$$\Psi_{k_d}^{(+)}(\mathbf{r}, \mathbf{R}) = \phi_d(\mathbf{r}) \chi_d^{(+)}(\mathbf{R}) + \int dk \phi_k(\varepsilon_k, \mathbf{r}) \chi_k^{(+)}(\varepsilon_k, \mathbf{R})$$

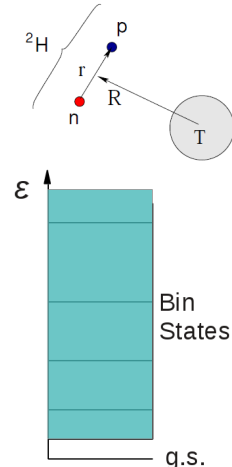
$$\Rightarrow \Psi_{k_d}^{(+)\text{CDCC}}(\mathbf{r}, \mathbf{R}) = \phi_d(\mathbf{r}) \chi_d^{(+)}(\mathbf{R}) + \sum_k \phi_k(\varepsilon_k, \mathbf{r}) \chi_k^{(+)}(\varepsilon_k, \mathbf{R}).$$

- The coupled equations:

$$(T_R + H_r + V_n + V_p) \sum_j \phi_j(\mathbf{r}) \chi_j^{(+)}(\mathbf{R}) = E \sum_j \phi_j(\mathbf{r}) \chi_j^{(+)}(\mathbf{R}).$$

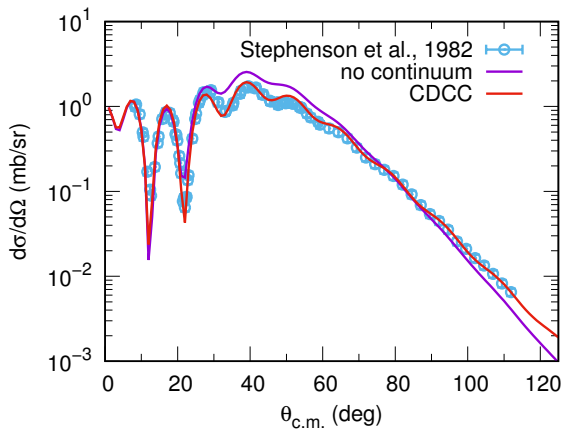
$$\Rightarrow (T_R + \epsilon_i - E + V_{ii}) \chi_i^{(+)}(\mathbf{R}) = - \sum_{j \neq i} V_{ij} \chi_j^{(+)}(\mathbf{R})$$

$$V_{ij}(R) = \langle \phi_i(\mathbf{r}) | V_n + V_p | \phi_j(\mathbf{r}) \rangle.$$

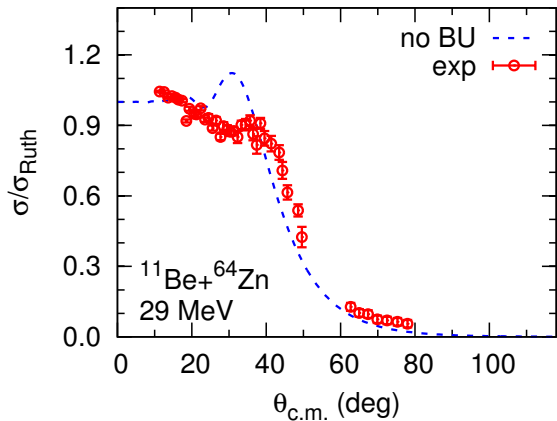


CDCC calculation: an example

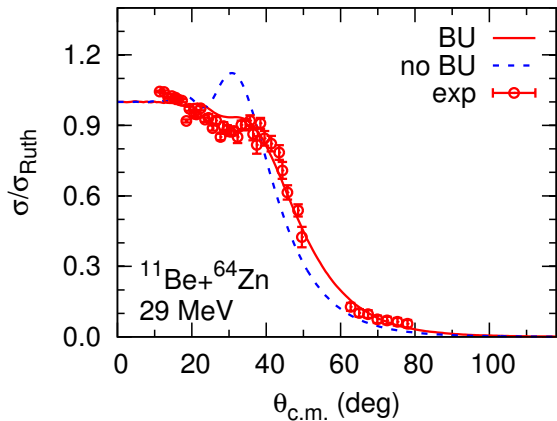
Elastic scattering of d+⁵⁸Ni at 79 MeV. Neutron, proton optical potentials from CH89.



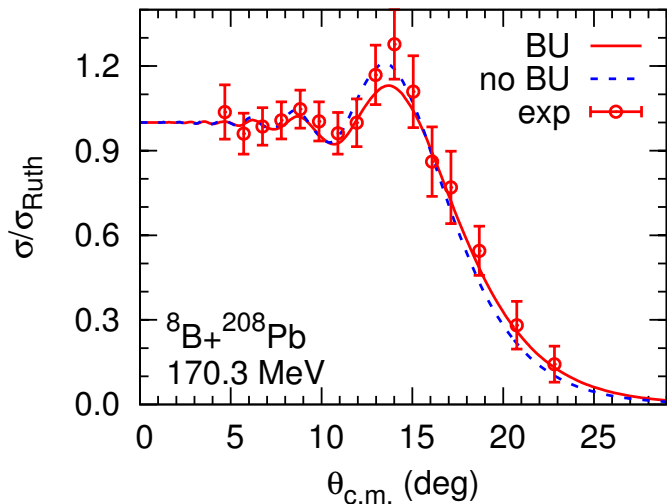
exp data: E.J. Stephenson et al, PRC 28, 134 (1983)

$^{11}\text{Be} + ^{64}\text{Zn}$ at 29 MeV

$E_{1n} = 0.502 \text{ MeV}$, A. Di Pietro PRL 105, 022701 (2010), PRC 85, 054607 (2012)

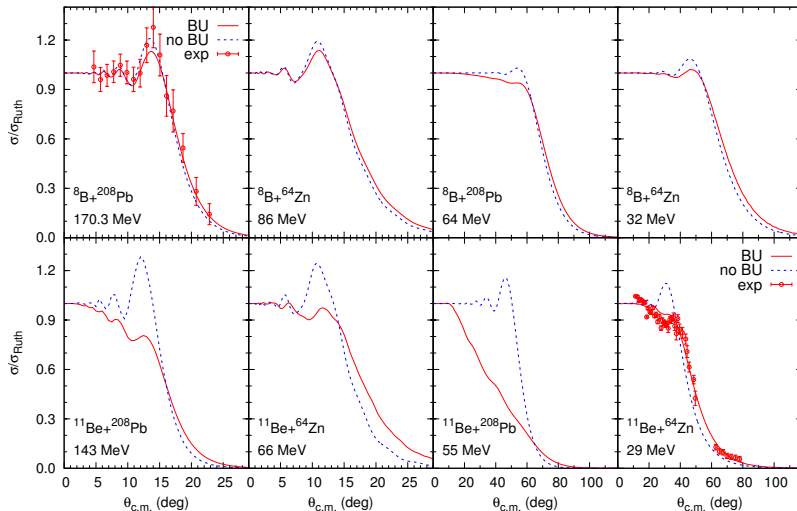
$^{11}\text{Be} + ^{64}\text{Zn}$ at 29 MeV

$E_{1n} = 0.502$ MeV, A. Di Pietro PRL 105, 022701 (2010), PRC 85, 054607 (2012)

${}^8\text{B} + {}^{208}\text{Pb}$ at 170.3 MeV

$E_{1p} = 0.138$ MeV, Yang Yan-Yun, Wang Jian-Song, et al., PRC 87, 044613 (2013)

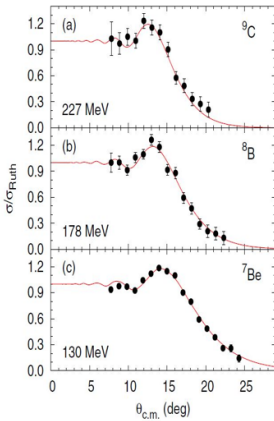
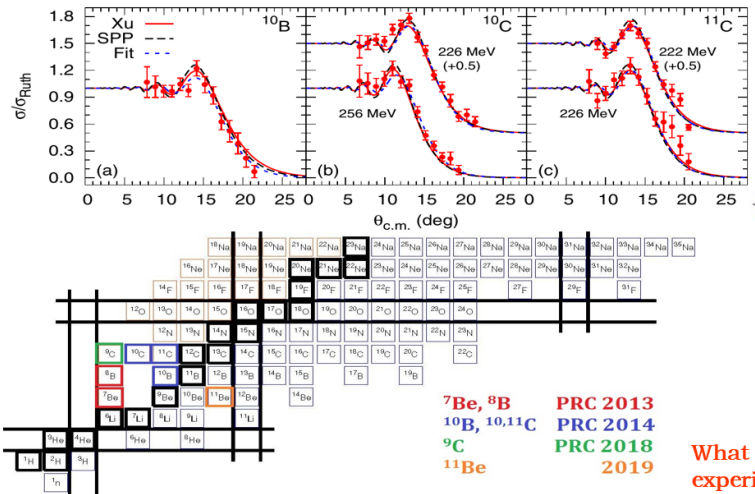
breakup coupling effects in the elastic scattering of ^8B and ^{11}Be



Y.Y. Yang, X. Liu, D.Y. Pang, PRC 94, 034614 (2016)

Experiments performed at IMP Lanzhou

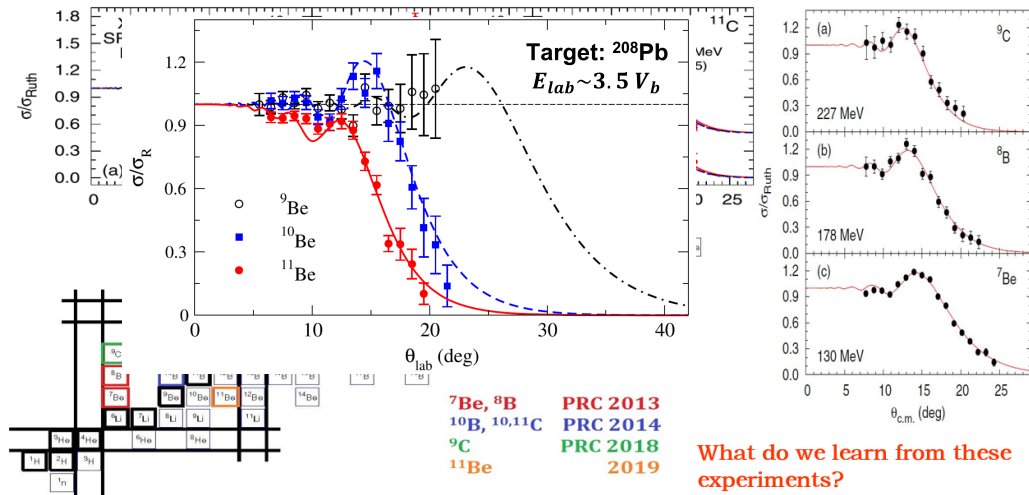
elastic scattering of weakly-bound nuclei: experiments performed at IMP Lanzhou



What do we learn from these experiments?

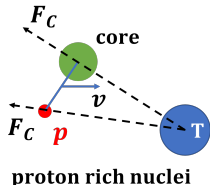
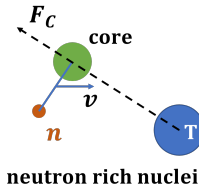
Experiments performed at IMP Lanzhou

elastic scattering of weakly-bound nuclei: experiments performed at IMP Lanzhou



Differences in n-rich and p-rich nuclei

- The tidal force:



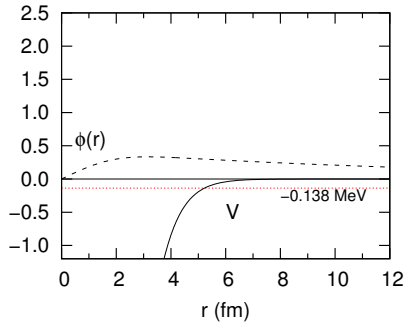
- The Schrödinger equation:

$$\left[-\frac{\hbar^2}{2\mu} \frac{d^2}{dr^2} + V_N + V_C + \frac{\hbar^2 \ell(\ell+1)}{2\mu r^2} \right] \phi_{nlj}(r) = \varepsilon \phi_{nlj}(r)$$

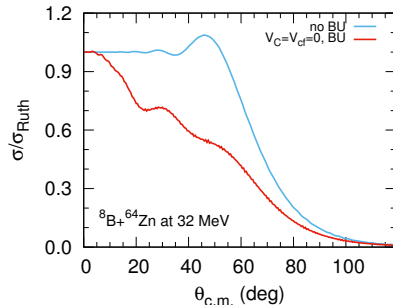
- Coulomb potential: $V_C(r) = \frac{Z_c e^2}{r}$, ($r > R$)
- The centrifugal potential: $V_{cf}(r) = \frac{\hbar^2 \ell(\ell+1)}{2\mu r^2}$

⁸B: $V_C \neq 0$, $V_{cf} \neq 0$ ($1p_{3/2} \Rightarrow \ell = 1$), ¹¹Be: $V_C = 0$, $V_{cf} = 0$ ($2s_{1/2} \Rightarrow \ell = 0$)

Effect of Coulomb and centrifugal barriers

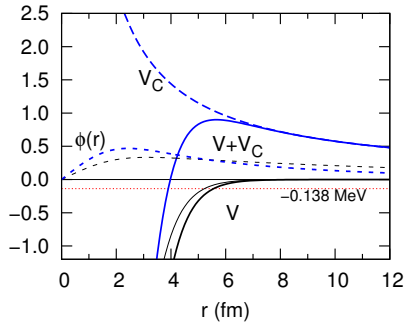


$$V_C = 0, V_{cf} = 0$$

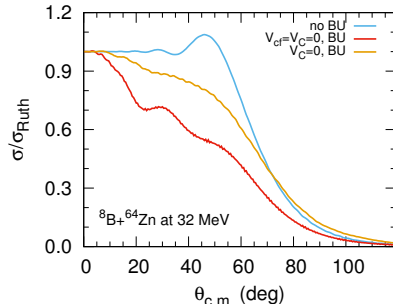


$$V_C = 0, V_{cf} = 0$$

Effect of Coulomb and centrifugal barriers

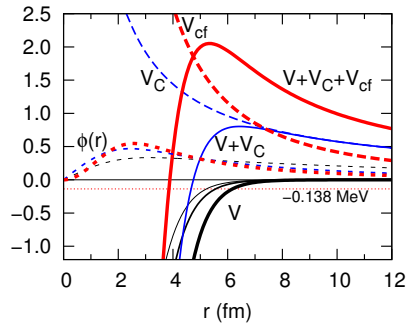


$$V_C = 0, V_{cf} \neq 0$$

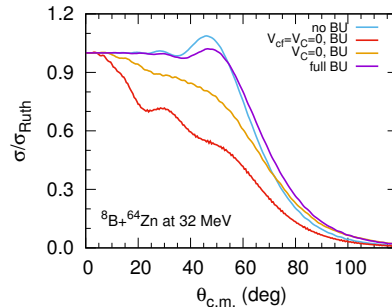


$$V_C = 0, V_{cf} \neq 0$$

Effect of Coulomb and centrifugal barriers



$$V_C \neq 0, V_{cf} \neq 0$$

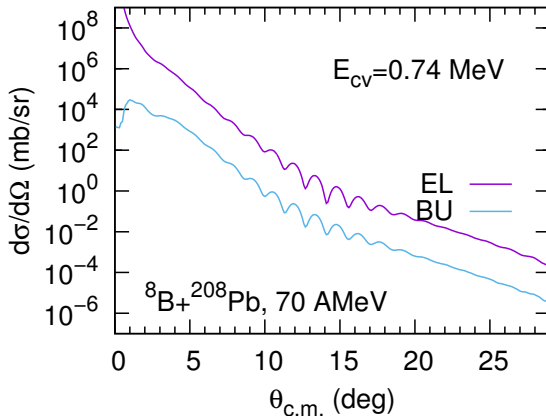
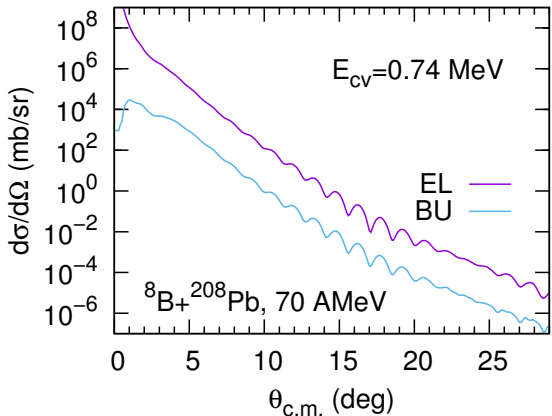


$$V_C \neq 0, V_{cf} \neq 0$$

Elastic scattering \Rightarrow single-particle structure!

elastic and breakup

Elastic scattering and breakup cross sections : depend on Optical model potentials



OMP parameters: LHS: $N_r = 0.72$, $N_i = 1.21$; RHS: $N_r = 0.80$, $N_i = 1.0$

Ratio of cross sections: weakly dependent on OMP

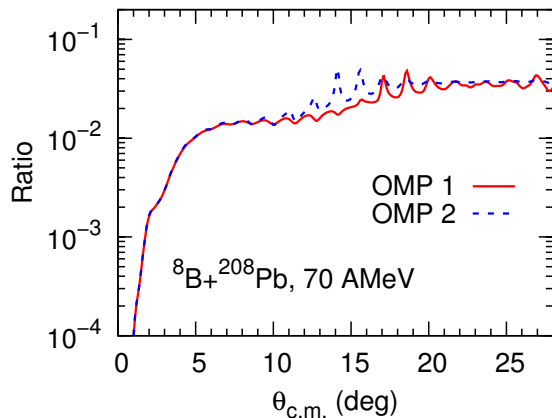
Ratio of breakup and elastic scattering cross sections depend weakly on OMP

The measured cross sections:

$$\frac{d\sigma_{\text{sum}}}{d\Omega} = \frac{d\sigma_{\text{el}}}{d\Omega} + \frac{d\sigma_{\text{inel}}}{d\Omega} + \int \frac{d\sigma_{\text{BU}}}{dE d\Omega} dE.$$

The ratio:

$$\mathcal{R}_{\text{sum}}(E, \mathbf{Q}) = \frac{d\sigma_{\text{BU}}/dEd\Omega}{d\sigma_{\text{sum}}/d\Omega}$$



The Recoil Eikonal breakup (REB) model

With **the Recoil Eikonal Breakup (REB) model** [Assumes V_{nT} is negligible and adiabatic approx., R. Johnson, J. Al-Khalili, J. Tostevin, PRL 79, 2771 (1997)]:

Elastic scattering:

$$\frac{d\sigma_{el}}{d\Omega} = |F_{00}|^2 \left(\frac{d\sigma}{d\Omega} \right)_{pt}$$

Form factor: $F_{00} = \int |\phi_0|^2 e^{i\mathbf{Q} \cdot \mathbf{r}} d\mathbf{r}$, $\mathbf{Q} \propto (\mathbf{K} - \mathbf{K}')$

⇒ Elastic scattering of composite nuclei = form factor × point-like particle scattering

Breakup cross sections: $\frac{d\sigma_{bu}}{dEd\Omega} = |F_{E0}|^2 \left(\frac{d\sigma}{d\Omega} \right)_{pt}$

Form factor: $|F_{E0}|^2 = \sum_{ljm} \left| \int \phi_{ljm}(E) \phi_0 e^{i\mathbf{Q} \cdot \mathbf{r}} d\mathbf{r} \right|^2$

⇒ similarity of elastic and breakup angular distributions

⇒ The **ratio method!**

The Recoil Eikonal breakup (REB) model

With **the Recoil Eikonal Breakup (REB) model** [Assumes V_{nT} is negligible and adiabatic approx., R. Johnson, J. Al-Khalili, J. Tostevin, PRL 79, 2771 (1997)]:

Elastic scattering:

$$\frac{d\sigma_{\text{el}}}{d\Omega} = |F_{00}|^2 \left(\frac{d\sigma}{d\Omega} \right)_{\text{pt}}$$

Form factor: $F_{00} = \int |\phi_0|^2 e^{i\mathbf{Q} \cdot \mathbf{r}} d\mathbf{r}$, $\mathbf{Q} \propto (\mathbf{K} - \mathbf{K'})$

\Rightarrow Elastic scattering of composite nuclei = form factor \times point-like particle scattering

Breakup cross sections: $\frac{d\sigma_{\text{bu}}}{dEd\Omega} = |F_{E0}|^2 \left(\frac{d\sigma}{d\Omega} \right)_{\text{pt}}$

Form factor: $|F_{E0}|^2 = \sum_{lm} \left| \int \phi_{lm}(E) \phi_0 e^{i\mathbf{Q} \cdot \mathbf{r}} d\mathbf{r} \right|^2$

\Rightarrow similarity of elastic and breakup angular distributions

\Rightarrow The **ratio method!**

The Recoil Eikonal breakup (REB) model

With **the Recoil Eikonal Breakup (REB) model** [Assumes V_{nT} is negligible and adiabatic approx., R. Johnson, J. Al-Khalili, J. Tostevin, PRL 79, 2771 (1997)]:

Elastic scattering:

$$\frac{d\sigma_{\text{el}}}{d\Omega} = |F_{00}|^2 \left(\frac{d\sigma}{d\Omega} \right)_{\text{pt}}$$

Form factor: $F_{00} = \int |\phi_0|^2 e^{i\mathbf{Q} \cdot \mathbf{r}} d\mathbf{r}$, $\mathbf{Q} \propto (\mathbf{K} - \mathbf{K'})$

⇒ Elastic scattering of composite nuclei = form factor × point-like particle scattering

Breakup cross sections: $\frac{d\sigma_{\text{bu}}}{dEd\Omega} = |F_{E0}|^2 \left(\frac{d\sigma}{d\Omega} \right)_{\text{pt}}$

Form factor: $|F_{E0}|^2 = \sum_{ljm} \left| \int \phi_{ljm}(E) \phi_0 e^{i\mathbf{Q} \cdot \mathbf{r}} d\mathbf{r} \right|^2$

⇒ similarity of elastic and breakup angular distributions

⇒ The **ratio method!**

The Recoil Eikonal breakup (REB) model

With **the Recoil Eikonal Breakup (REB) model** [Assumes V_{nT} is negligible and adiabatic approx., R. Johnson, J. Al-Khalili, J. Tostevin, PRL 79, 2771 (1997)]:

Elastic scattering:

$$\frac{d\sigma_{\text{el}}}{d\Omega} = |F_{00}|^2 \left(\frac{d\sigma}{d\Omega} \right)_{\text{pt}}$$

Form factor: $F_{00} = \int |\phi_0|^2 e^{i\mathbf{Q} \cdot \mathbf{r}} d\mathbf{r}$, $\mathbf{Q} \propto (\mathbf{K} - \mathbf{K'})$

\Rightarrow Elastic scattering of composite nuclei = form factor \times point-like particle scattering

Breakup cross sections:

$$\frac{d\sigma_{\text{bu}}}{dEd\Omega} = |F_{E0}|^2 \left(\frac{d\sigma}{d\Omega} \right)_{\text{pt}}$$

Form factor: $|F_{E0}|^2 = \sum_{ljm} \left| \int \phi_{ljm}(E) \phi_0 e^{i\mathbf{Q} \cdot \mathbf{r}} d\mathbf{r} \right|^2$

\Rightarrow similarity of elastic and breakup angular distributions

\Rightarrow The **ratio method!**

The ratio method

With the REB model:

$$\frac{\sigma_{\text{bu}}}{\sigma_{\text{el}}} = \frac{|F_{E0}(\mathbf{Q})|^2}{|F_{00}(\mathbf{Q})|^2}$$

- Independent on **reaction mechanisms**: nuclear or Coulomb breakup, light or heavy targets
- Directly related to the **single-particle structure of projectile**
- **Easy to measure**: many systematic uncertainties canceled

Johnson, Al-Khalili and Tostevin, PRL 79, 2771 (1997); Capel, Johnson, Nunes, PLB 705, 112 (2011), ibid, PRC 88, 044602 (2013); Yun, Colomer, Capel, and Pang, JPG 46, 105111 (2019).

The ratio: weak dependence on target masses

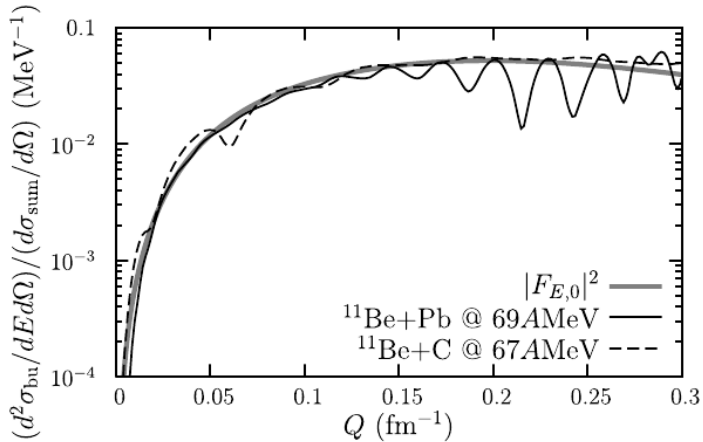


Fig. 4. Sensitivity of ratio (4) to the reaction mechanism. DEA calculations on different targets are compared to $|F_{E,0}|^2$.

The ratio: sensitive to binding energies

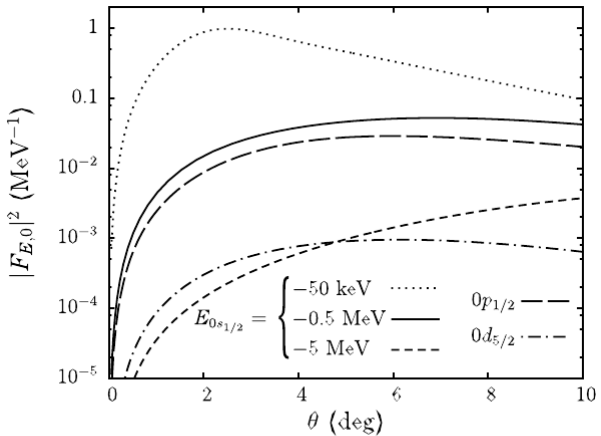
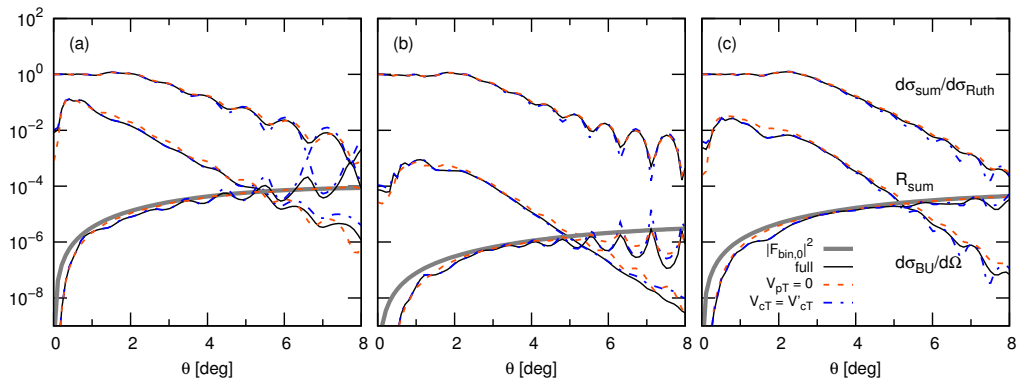


Fig. 1. Form factor $|F_{E,0}|^2$ for ^{11}Be impinging on Pb at 69 MeV/nucleon. Its sensitivity to the projectile binding energy and partial-wave configuration is illustrated.

The ratio method: applicability for proton-rich nuclei



^{17}F (a), ^{25}Al (b) and ^{27}P (c) from ^{58}Ni at 60 MeV/n, breakup/elastic ratios and the FFs.
 Proton separation energies: ^{17}F : 0.6 MeV ($1d_{5/2}$), ^{25}Al : 2.27 MeV ($1d_{5/2}$);
 ^{27}P : 0.87 MeV ($2s_{1/2}$)

Yun, Colomer, Capel, and Pang, JPG 46, 105111 (2019)

Breakup induced dynamic polarization potentials

- The coupled equations:

$$(T_R + \epsilon_i - E + V_{ii})\chi_i^{(+)}(\mathbf{R}) = - \sum_{j \neq i} V_{ij}\chi_j^{(+)}(\mathbf{R})$$

- For the elastic scattering channel ($i = 0$):

$$\Rightarrow \left(T_R + \epsilon_i - E + V_{00} + \underbrace{\frac{\sum_{j \neq i} V_{ij}\chi_j^{(+)}(\mathbf{R})}{\chi_i^{(+)}(\mathbf{R})}}_{\chi_0^{(+)}(\mathbf{R})} \right) \chi_0^{(+)}(\mathbf{R}) = 0$$

- The **dynamic polarization potential**:

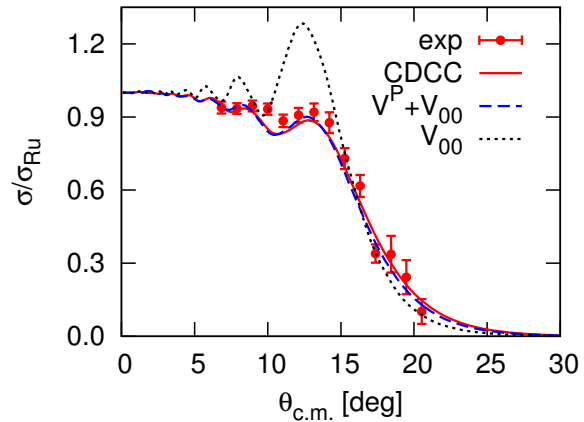
$$V^P(R) \equiv \frac{\sum_{j \neq i} V_{ij}\chi_j^{(+)}(\mathbf{R})}{\chi_i^{(+)}(\mathbf{R})}$$

- We get a 1-channel equation with $U(R) = V_{00} + V^P$ (V_{00} : **bare potential**):

$$\Rightarrow [T_R + \epsilon_i - E + U(R)] \chi_0^{(+)}(\mathbf{R}) = 0$$

Breakup induced dynamic polarization potentials

Example: $^{11}\text{Be} + ^{208}\text{Pb}$ elastic scattering at 140 MeV.



Li Yan, D.Y. Pang, Eur. Phys. J. A 57, 46 (2021).

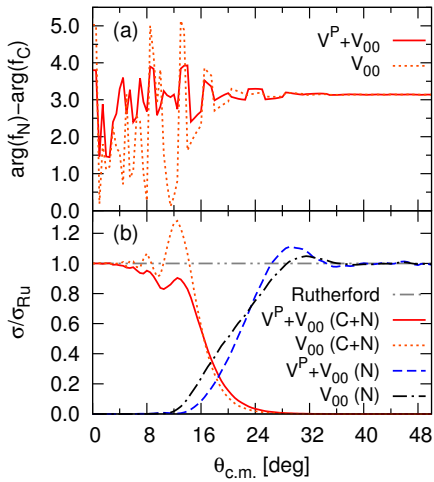
Breakup induced dynamic polarization potentials

Example: $^{11}\text{Be} + ^{208}\text{Pb}$ elastic scattering at 140 MeV.

$$\frac{d\sigma}{d\Omega} = |f(\theta)|^2$$

$$f(\theta) = f_C(\theta) + f_N(\theta)$$

⇒ The breakup channels cause a destructive interference between the Coulomb and Nuclear amplitudes at angles where the Coulomb-nuclear interference peak used to be.



Li Yan, D.Y. Pang, Eur. Phys. J. A 57, 46 (2021).